LABORATORY TESTING AND FINITE ELEMENT MODELING OF INVERT REMOVED CORRUGATED METAL CULVERT BURIED UNDER SHALLOW COVER

by

HIRAMANI RAJ CHIMAURIYA

Presented to the Faculty of the Graduate School of

The University of Texas at Arlington in Partial Fulfillment

of the Requirements

for the Degree of

MASTER OF SCIENCE IN CIVIL ENGINEERING

THE UNIVERISTY OF TEXAS AT ARLINGTON

August 2019

ACKNOWLEDGEMENT

First and foremost, I would like to express my sincerest thanks and gratitude to my research advisor Dr. Xinbao Yu for providing me with this invaluable opportunity to work under his guidance. I can confidently state that without his continuous support and guidance, this research would never have been possible. I count myself extremely lucky to have had this opportunity to pursue by master's degree under his guidance.

I would also like to thank Dr. Sahadat Hossain, Dr. Mohammad Najafi and Dr. Himan Hojat Jalali for agreeing to be a part of my thesis committee and providing me with valuable suggestions and ideas to better my work. I am thankful to Dr. Najafi and the Center for Underground Infrastructure Research and Education (CUIRE) at the University of Texas at Arlington for letting me be a part of this project and helping me with its execution. This research was conducted under a pool-funded project from National Cooperative Highway Research Program (NCHRP) at CUIRE. I would like to thank Ohio Department of Transportation (Ohio DOT) for leading the project and six other DOTs including DelDOT, FDOT, MnDOT, NCDOT, NYSDOT and PennDOT for funding and contributing to this project. I would like to thank partner companies and consultants, LEO Consulting, LLC, Rehabilitation Resource Solutions, LLC, and American Structurepoint, Inc. In addition, Contech Engineering, Forterra Pipe and Precast, Madewell Products Corporation, Strong Products, HVJ Associates and Braun Intertec for providing us with various products and services that were most essential for these tests.

A special shout out to my friends Samrat Raut, Amin Darabnuoush Tehrani, Juhil Jitendra Makwana and Shobhit Srivastava for their hard work and support. Without their hard work and strong work ethic, these tests could never have been accomplished. I would also like to thank Seyedmohammadsadegh Jalalediny Korky, Ramtin Serajiantehrani and Zahra Kohankar Kouchesfehani for their contributions to this project.

I am always grateful to my parents for their continuous inspiration and support. They have encouraged me through some of the toughest times, and I owe all I have achieved to them. I am also grateful for my friends, both old and new, who have helped make this place a home away from home. Thank you!

August 12, 2019

ABSTRACT

LABORATORY TESTING AND FINITE ELEMENT MODELING OF INVERT REMOVED CORRUGATED METAL CULVERT BURIED UNDER SHALLOW COVER

Hiramani Raj Chimauriya

The University of Texas at Arlington, 2019

Supervising Professor: Dr. Xinbao Yu

Ever since their advent in the 1800s, corrugated metal pipes (CMPs) have played a vital role in this nation's infrastructure. The wide range of options on diameter and span have made these culverts more preferable over traditional concrete culverts. However, compared to concrete culverts, CMPs have a shorter design life and are only expected to last 10 to 30 years even under ideal conditions. Over the course of years, different open-cut and trenchless methods have been used to rehabilitate existing old and damaged culverts. In recent years, trenchless methods like sliplining, CIPP, spray-applied pipe linings, etc. have been gaining popularity over open-cut methods as they are quicker, easier to install and prevent economic costs incurred from having to block road traffic over the duration of repairs. In addition to this, rehabilitation methods like CIPP and spray applier linings can benefit significantly from the residual capacity of host pipes. However, this residual capacity is usually ignored when designing such repair methods. One of the reasons for this is because of the difficulty in determining the residual capacity of a damaged culvert. Therefore, if this residual capacity could be properly defined, it can be used to design more efficient and economic rehabilitation methods.

In this thesis, laboratory tests and finite element modeling are used to identify the residual capacity of a damaged CMP. Damage to the culvert's invert due to corrosion and abrasion was found to be the most common form of damage among CMPs. There have been studies in the past that have tried to simulate damaged culverts by reducing the wall thickness in finite element (FE) models or testing deteriorated culverts exhumed from field. However, due to the varying degree and distribution of corrosion in tested culverts, the data cannot be reliably used to quantify the residual capacity of a damaged CMP. Because of this difficulty in maintaining the same degree of control over the damage parameters, CMPs with removed invert are tested to obtain the residual capacity of damaged culverts. This is considered as the worst-case scenario and the base line data obtained from this test can be conservatively used to design suitable repair and rehabilitation practices. To obtain the measure of the residual capacity, an intact CMP is tested for baseline data. Both the CMPs are analyzed under a shallow cover to reduce

the load distribution provided by the soil and hence further simulate rare but critical field condition.

The laboratory test on intact CMP showed that under shallow cover, with a standard AASHTO H20 truck's footprint sized load pad, the failure mode is local buckling in pipe. The failure of cover soil was seen prior to buckling. However, the system easily handled the H20 service load of 16,000 lbs. without significant deformations to CMP. The finite element model of the test mimicked the test's response fairly well up to the point of soil failure. Once failure of soil occurred, further response could not be modeled as the numerical solutions did not converge beyond this state. For invert-cut CMP, the failure mode was excessive deformation. This deformation was highest at the location of the removed invert (haunch), with the CMP moving inwards to reduce the gap. The invert-cut CMP was significantly weaker than the intact CMP and the maximum pressure capacity was reduced by over 91%.

LIST OF ACRONYMS

ASTM: American Society of Testing and Materials.

AASHTO: American Association of State Highway and Transportation Officials.

CHBDC: Canadian Highway Bridge Design Code.

CMP: Corrugated Metal Pipe.

CIPP: Cured-in-place Pipe Lining.

FE: Finite Element.

FEM: Finite Element Model.

FHWA: Federal Highway Administration.

HDPE: High Density Polyethylene.

PVC: Polyvinyl Chloride.

SAPL: Spray Applied Pipe Liners.

USBR: United States Bureau of Reclamation.

USCS: United Soil Classification System.

TABLE OF CONTENTS

LIST OF FIGURES

LIST OF TABLES

Chapter 1 INTRODUCTION

1.1 Introduction

From ancient Roman aqueducts to modern storm water culverts, pipes have played a major role in the development of human civilization. Hence, it is to be expected that as the civilization and available technology advances, the advancements in the field pipelines also moved ahead. Among the various advancements made in this field, one of the most important is the development of corrugated metal pipes (CMPs). Developed in 1896, these pipes provided a wide a range of shape and size options with installations over 50 feet in diameter and 80 feet of span made possible (National Corrugated Steel Pipe Association 2008).

Generally, corrugated metal pipes are considered to have a service life of 10 to 35 years provided no perforations occur (Rinker Materials 1994). However, once perforations are found in a culvert, the highest rating it can have according to the FHWA culvert inspection manual is three, which is very close to the critical rating of zero. Any culvert that receives a critical rating is supposed to be immediately replaced (Arnoult 1986). Having been in service for so long, it is not surprising that many of the corrugated metal culverts in the US have suffered significant damage and are in need of repair or replacement. Timely repair and rehabilitation of culverts can prevent the additional time and cost that would be incurred should emergency exhumation and replacement of the culvert be needed due to critical damage.

Figure 1-1: 9 ft. diameter CMP with corrugated invert on Elba Township in Knox County, III (Miliken Infrastructure Solutions 2016).

There are several trenchless methods available that are being used to repair and rehabilitate deteriorated culverts, hence saving the increase in cost and disruption due to replacement of damaged culverts using traditional open-cut methods. These methods include installing or renewing underground utility systems with minimum surface or subsurface disruptions (Najafi and Gokhale 2005). Some of the more popular options are sliplining, cured-in-place pipe lining (CIPP), fold-and-form lining, spiral-wound lining and spray applied pipe lining (Matthews et al. 2012).

Figure 1-2: Culvert rehabilitation using (left to right): sliplining (DEWCON Infrastructure Rehabilitation 2019), fold-and-form lining and spiral wound lining (Matthews et al. 2012).

Repair methods like sliplining, fold-and-form lining and spiral-wound lining have different design standards and practices but the common theme is that the design capacity of these methods does not rely on the residual capacity of host pipes and instead are intended to act as stand-alone culverts that can handle the design load i.e., they can have same design irrespective of the levels of deterioration in host pipe. Cured-in-place pipe lining (CIPP) can be designed for both partial and full deterioration. The current practice defines partial deterioration as the state where the surrounding soil still provides

adequate support to the culvert and can still support the soil and surcharge loads adequately for its entire design life. Therefore, in cases of partial deterioration, the CIPP is only designed to support the hydrostatic loads due to groundwater i.e., it takes into account the residual capacity of the host culvert. However, in cases where the parts of the culvert have been lost due to corrosion or soil loads, etc., the culvert is considered fully deteriorated and the CIPP is designed to take the full design hydrostatic, soil or surcharge loads (ASTM 2016). Hence, any residual capacity of the host structure is ignored. Spray applied pipe liners, theoretically, benefit from the residual capacity of the host structures due to composite action and there have been limited studies conducted into the behavior and contribution of SAPLs in rehabilitating a culvert (Kouchesfehani et al. 2019; Syar et al. 2019; Tehrani et al. 2019). However, there are no design standards as of yet that can quantify this capacity and hence the use of spray applied pipe liners has largely been at the discretion of vendors or the clients that use them.

Figure 1-3: Pipe repair using (left to right): CIPP and spray applied liner (Matthews et al. 2012).

1.2 Problem Statement

There are many existing methods available to rehabilitate a culvert, each with its own sets of advantages and disadvantages. However, the improvement in strength/capacity due to the various rehabilitation methods has not always been clearly identified. This is especially true in cases of rehabilitation using spray-applied pipe liners where the host structure can provide significant addition to the strength provided by the liner itself. Whenever a rehabilitation method is applied for full structural rehabilitation of an existing culvert, the contributions of the host pipe are usually neglected to obtain conservative values under the assumption that, somewhere soon along the road, the culvert will become fully deteriorated. However, as various field studies and inspections have shown, a culvert does not deteriorate uniformly i.e., the deterioration is not the same over the entire cross-section. Instead, the damage is almost disproportionately concentrated to the areas around the invert (between the two haunches) (Moore and

Becerril Garcia 2015; Matthews et al. 2012; Mai et al. 2014; Mai 2013; Mai et al. 2013; Becerril García and Moore 2015; Ballinger and Drake 1995; Arnoult 1986; USBR 1998; Sargand et al. 2018). Therefore, if complete invert removal is considered as a worst-case scenario, determining the loss in strength and stability of the host structure in this scenario can help better optimize the repair and rehabilitation efforts of the culvert by accounting for the contributions of the intact portions of the host structure on providing additional strength to the rehabilitated culvert. Hence, this study is concerned with comparing the behavior of intact and invert removed culvert to quantify the residual capacity of a host culvert that has undergone severe deterioration and is in need of rehabilitation or replacement through laboratory test and finite element analysis.

1.3 Research Objective

The main objective of this study is to quantify the residual capacity of a corrugated metal pipe (CMP) with no invert. The specific objectives of the study are as follows:

- Perform full-scale laboratory test on a buried intact CMP sample to obtain a baseline data.
- Perform full-scale laboratory test on a buried CMP sample without invert to obtain residual capacity of the CMP.
- Perform finite element analysis simulating the laboratory test.

1.4Thesis Organization

The thesis is divided into five chapters. Chapter 1 is the introduction section and it introduces the topic, nature of the problem, purpose of study and organization on this thesis.

Chapter 2 consists of the literature review performed over the course of the study. Information about the past and present design procedures, commonly seen deterioration and other relevant studies is presented in this section.

Chapter 3 provides details about the laboratory test performed on intact and invert removed CMP.

Chapter 4 details the finite element analysis of the laboratory test. Information about the type of model, necessary tests performed to obtain soil properties and model verification is included in this chapter.

Chapter 5 is the conclusions chapter. It summarizes the entirety of the works performed, draws conclusions based on the observed results and provides recommendation for future studies.

Chapter 2 LITERATURE REVIEW

2.1 Introduction

Corrugated metal pipes (CMPs) are flexible in nature. Hence, unlike rigid concrete pipes, these pipes are expected to deflect under load. Therefore, had the stability of such systems been a function of the pipe alone, CMPs would not be able to function as pipes under any practical load. Instead, CMPs, or indeed any flexible pipes, derive a significant portion of their strength and stability through the support provided by the surrounding soil. Figure 2-1 shows the assumed distribution of soil pressure around the pipe that adds to the pipe's resistance to applied loads. If the pipe starts to deflect, the soil around it tries to deflect as well and develops passive resistance against any further deformation. Hence, if the backfill soil is strong, the pipe receives greater support. This pipe-soil interaction is the reason why CMP design or repair is such an interesting as well as challenging problem. For example, if a CMP suffering from extreme corrosion develops perforations in some places, the flow inside the CMP leaks to the surrounding soil. This can induce piping and eventual erosion, leading to formation of voids around the pipe-soil interface. This in turn will reduce the support to the pipe and hence accelerate the damage to it. Conversely, if the soil around the pipe is of poor quality, the resistance it provides to the pipe against deflection is reduced which can cause excessive deformation, localized buckling or even collapse of the system. Similarly, the factors like chemical makeup and ground water levels of the backfill soil can corrode the pipe from the outer surface as well. Hence, when looking at the stability of a buried CMP, it is of utmost importance to never neglect the soil surrounding it. This fact has long been identified in the pipe community. Thus, this section provides information gained from various literatures regarding the process of design of CMPs, common failure modes and relevant studies that have been conducted in the past to further the knowledge in this field.

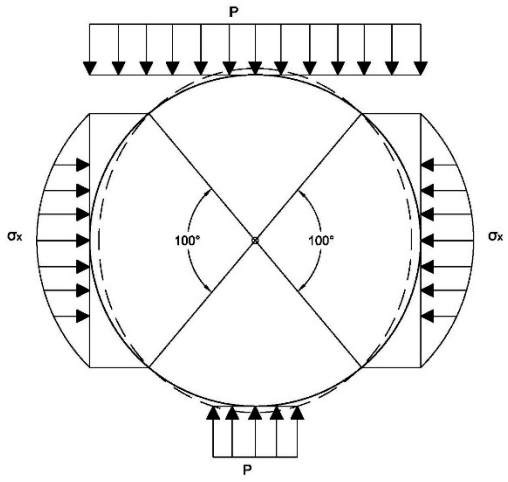

Figure 2-1: Assumed pressure distribution around the pipe for Iowa Formula (Whidden 2009).

2.2 Design History of CMPs

Despite their immense value and contribution to the advancement of society, the design of pipes had, for a long time, been empirical and based on field experiences. The major contribution in design of buried pipes was first provided by Anson Marston on 1913 (McGrath et al. 2018; Whidden 2009). He developed an equation based on the soil load on the pipe. This “Marston Load” was used as the design load that had to be met by the three-edge bearing test of pipe. This design method was successfully used as the standard for concrete pipes. However, at the advent of corrugated steel pipes (CMPs), it was found that these pipes could not handle the Marston load during a three-edge bearing test. This lead Spangler (1941) to study the behavior of these pipes and develop the concept of soil-structure interaction. Considering the effects of soil-structure interaction, Spangler developed the Iowa Formula for predicting the horizontal expansion of buried, flexible pipes (Spangler 1941). However, this formula was not successful in sufficiently representing the pipe behavior. Watkins and Spangler further studied the relation and found that the inaccuracies were due to incorrect definition of horizontal soil modulus (Watkins and Spangler 1958). They modified the relation and developed the Modified Iowa Formula in the form of equation 2.1:

$$\Delta x = \frac{D_f K W_c r^3}{EI + 0.061 E' r^3} \qquad 2-1$$

where,

Δx= increase in horizontal diameter (in.),
D_f= deflection lag factor (about 1.0),
K= bedding factor (about 1.0),
W_c= PD= Marston load on the pipe (lb/in.),
P= soil pressure on top of the pipe,
D= pipe diameter (in.),
r= pipe radius= D/2 (in.),
E= modulus of elasticity of pipe (psi),
I= $t^3/12$ for plain pipe wall ($in.^4/in.$),
t= wall thickness (in.), and
E’= modulus of elasticity of soil (psi).

The vertical ring deflection is then calculated using an adjusted form of the Iowa formula as:

$$d = \frac{\Delta}{D} \qquad 2-2$$

$$d(\%) = \frac{10P}{\Sigma\left(\frac{EI}{r^3}\right) + 0.06E'} \qquad 2-3$$

where,

d = ring deflection ratio=∆y/D, where ∆y is the vertical decrease in diameter;
E = modulus of elasticity of the pipe material (psi);
E'= horizontal modulus of soil reaction (psi).

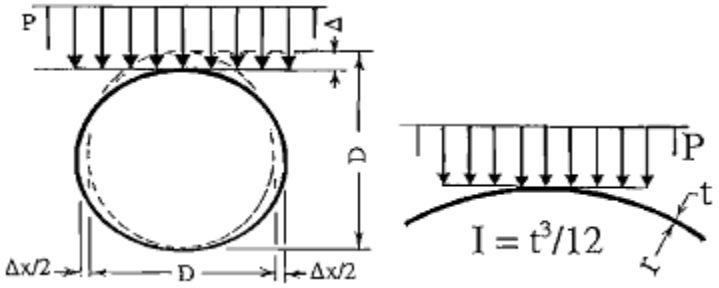

Figure 2-2: Expressions for ring deflection, d (Whidden 2009)

The denominators in the above equation represent the effects of soil and pipe where, E' is the soil stiffness and EI/r^3 is the ring stiffness. The adjusted form of Iowa formula clearly shows that the ring deflection of the pipe is primarily the function of soil embedment. There have also been several further studies and research that have concluded that the strength/stability of buried flexible pipes comes from the horizontal soil support which is developed when the pipe deflects under soil load (Katona and Akl 1978; McGrath et al. 2018; National Corrugated Steel Pipe Association 2008). However, that being said, the structural integrity of the original "host" pipe is still an important factor when considering the stability of the entire soil-structure system. In addition to retaining the shape, the host pipe also prevents the seepage of water into the surrounding soil, which in addition to being a stability concern, can also be an environmental issue depending on the type/chemical makeup of flow within the pipe.

2.3 Current Design Sequence

As has been amply verified by past studies in the field, the stability of a buried pipe is not a single component problem i.e., it is not solely dependent on the properties/behavior of the pipe. Instead, it is a complex soil-structure interaction problem where both components (soil and pipe) play a vital role. Hence, any design procedure for such system must also be able to account for the effect of the pipe-soil system in addition to the individual components themselves such that they can adequately meet the performance standards with a reasonable safety margin (i.e., factor of safety). Generally, the measure of performance in a soil-pipe system is deformation (as a function of loads, geometry and material properties) beyond which, the pipe-soil system cannot serve its intended purpose. More often than not, excessive deformation in pipes (causing leaks,

reduced flow capacity, etc.), which prevents the pipe from performing its intended function is considered as the performance marker for soil pipe systems (Watkins and Anderson 1999; Whidden 2009). Therefore, the most common performance limit for the pipe-soil system is taken as the deformation beyond which, the pipe cannot resist any increased load (Watkins and Anderson 1999). In case of external soil pressure, pipes can reach this performance limit in various ways, depending on the type of pipes as well as the surrounding soil (Figure 2-3). For flexible pipes like a CMP, the mode of failure can either be due to wall buckling or ring deflection, depending on the quality of backfill soil. In these cases, even though the soil itself can take the increased load, the system is still considered to have reached its performance limit or “failure” as the pipe no longer contributes to the system.

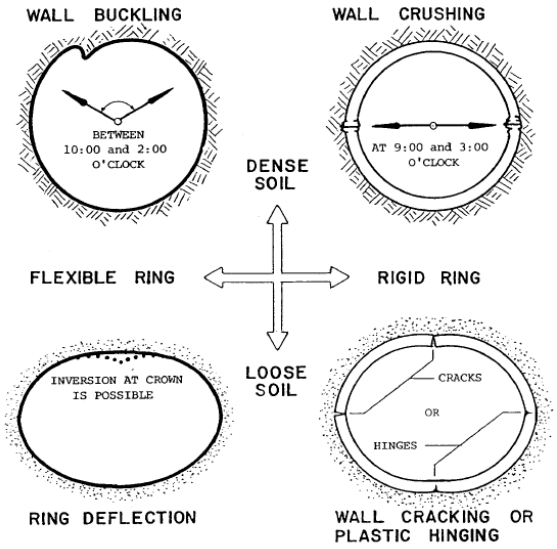

Figure 2-3: Typical ring failure conditions for buried pipes due to externals soil pressure (Watkins and Anderson 1999)

Generally, the design of buried pipes follows the following sequence:

1. Determination of pipe sizes and materials for adequate hydraulic performance.
2. Determination of minimum wall thickness for resisting internal pressure.
3. Determination of minimum ring stiffness for stability during handling and installation.
4. Determination of ring stiffness and soil strength required to resist external pressure.
5. Determination of ring stiffness and soil strength required to resist excessive ring deflection.
6. Longitudinal stress analysis.
7. Special design cases.

2.4 Deterioration of CMPs

Corrugated Metal Pipes, like anything else, are designed for a certain design life. However, as has been stated in previous sections, design of CMPs is a fairly new concept that is still being studied and improved on. Moreover, due to the vital role of the surrounding soil in the overall stability of the CMP, not all CMPs can successfully function throughout their design life without the need for maintenance, repairs or rehabilitation. Generally, a culvert requires rehabilitation or replacement for three major reason viz. due to bedding deficiencies, due to insufficient hydraulic capacity or due to insufficient structural capacity (Matthews et al. 2012). Each of these deficiencies are briefly discussed in the following sections.

2.4.1 Insufficient hydraulic capacity

Insufficient hydraulic capacity can mean either the hydraulic capacity of the existing culvert has reduced or the flow demand on the culvert has increased. As the culvert's age increases, it is more likely that its hydraulic capacity has reduced. This can happen in many ways like accumulation of debris in the invert, increase in friction loss due to surfaces abraded due to sliding and bumping of larger debris, etc. If the loss in capacity is due to increased friction loss, accumulation of debris, the capacity can be regained by performing routine maintenance. However, if the flow demand itself has increased, the existing culvert needs to be replaced using either traditional open-cut methods or trenchless methods like pipe splitting.

2.4.2 Deficiencies in bedding

In a pipe-soil system, bedding deficiencies can cause serious problems that can range from small depressions on the surface all the way to total collapse of the system. Bedding deficiencies can occur due to factors like piping or internal erosion, leaks in the culverts through joints, insufficient compaction during installation, etc. Internal erosion can also occur when the flow leaks from perforated regions in culvert. Provided that the cause of deficiencies in bedding are not due to the compromised structural integrity of the culvert, they can be fixed using methods like grouting. Internal erosion as the result of piping action can be prevented if the backfill soil is properly compacted during installation. However, if the cause for deficiencies is the leaks from the culverts itself, the culvert needs to be repaired for any other solution to have a lasting effect.

2.4.3 Insufficient structural capacity

Insufficient structural capacity is the most common cause of damage in culverts. When a culvert reaches insufficient structural capacity, it can no longer support the expected loads on it. The loss in structural capacity may be due to joint deficiencies (separated joints, offset joints, faulted joints, etc.) or due to damage to culvert walls due to corrosion and abrasion or, in extreme cases, the complete collapse of sections of the culvert. This study is geared towards the stability of a continuous/monolithic pipe structure and does not go into the study of joint defects. Loss due to complete/partial collapse of the culvert has also not been considered as no repair is possible and the

culvert will have to completely replaced in such cases. Hence, this study is focused on the loss of structural capacity due to damage to culvert walls.

According to Federal Highway Administration (FHWA), the most common damage seen in buried corrugated metal pipes/culverts are joint defects, shape distortion and invert loss (Ballinger and Drake 1995). Shape distortion of a CMP can be seen during the initial installation and handling of the pipe which may be either due to poor design (insufficient ring stiffness) or improper handling practices. Shape distortion seen in old CMPs can also be the function of long-term stresses experienced by the CMP throughout its service life. However, taking into account the fact that a CMP is a flexible structure and derives most of its strength from the surrounding soil, with proper design and installation, shape distortion can be a fairly manageable problem under normal conditions. Invert loss, on the other hand, is one of the most common (and hence the most severe) problems faced by CMPs during their design/service life (Matthews et al. 2012; Arnoult 1986; Ballinger and Drake 1995; García and Moore 2015; Mai et al. 2013; Masada 2017; Sargand et al. 2018; etc.). Numerous field inspections and studies on repairs on old CMPs have found that disproportionate amount of damage on a CMP has been concreted in the invert region, between the two haunches. The most common cause for this damage is the corrosion of invert due to the flow inside the CMP. However, it can also be caused by the abrasive action of debris dragged through the invert during times of insufficient flow.

Figure 2-4: Invert damage due to abrasion (left) and corrosion (right) (Matthews et al. 2012)

2.5 Relevant Laboratory and Field Tests

There have been various past studies that have studied the behavior of corrugated metal pipes under various conditions. This section summarizes a few of these studies that have bearings in this research.

Howard (1972) performed laboratory load tests on buried, bare steel pipes under clay cover and subjected to surcharge loads. The lean clay backfill soil was compacted to 95 to 100% of its standard proctor maximum dry density. The pipes tested had three

diameters: 18-, 24- and 30-in., with three different thicknesses (7, 10 and 14 gage) for each diameter. Four of the pipes buckled elastically at vertical deflections of less than 8%. Test on the other pipes after 10 psi of surcharge were found to produce good correlations with the Iowa formula. The differences seen during the initial loading were assumed to be caused by frictional resistance between soil and container walls. Near failure loads, the slope of load deflection curve was found to be dependent on the ring stiffness factor (EI/r^3) of the pipe. The experimental results were used to back calculate for the value of soil modulus (E') in the Iowa formula for different compaction levels. This study provided an important steppingstone for evaluating the limiting factors for flexible pipe design as well as modeling the pipe soil interaction.

Sharma et al. (2013) performed full scale laboratory tests on large diameter plain steel pipes buried under soil native to DFW, Texas and the same soil stabilized with lime to study the performance of different embedment soil. The pipe was 20 ft long with 72 in. diameter. Baseline data was obtained by burying the pipe under native soil up to 1 ft cover above pipe. Static dead load was then applied by adding 7 ft of pea gravel to the top. This was then compared with another test performed with same setup but using lime stabilized soil up to the springline of the pipe. Lime treatment was found to have improved the strength of the native soil and hence, reduced the pipe deflection.

Kunecki and Kubica (2004) performed full-scale laboratory tests and FEM analysis of corrugated steel culverts under standardized railway load. The study studied the response of the culvert under soil cover varying from 0.3 to 1 m. However, only the results obtained at 0.8 m soil cover were presented in the paper. The loads were applied using two hydraulic actuators transferred to the soil through two layers of wooden sleepers and steel plate. The test was then simulated using Cosmos/M system. The model's displacement showed good match to the experimental results however, the stresses were not in good agreement. This was attributed to the fact that the stiffness of retaining walls played an important role in the stress distribution around the soil and culvert which was not properly represented in the model.

Arockiasamy et al. (2006) performed several full-scale field tests on flexible pipes under vehicle load. The pipes tested were made of high-density polyethylene (HDPE), polyvinyl chloride (PVC) and metal and had two different diameters: 36 in. and 48 in. Tandem dump truck and FDOT truck filled with concrete blocks were used to simulate the load. The pipes were evaluated under 0.5D, 1D and 2D burial depths. The study demonstrated that with a 6 in. increase in cover thickness, the vertical soil pressure at the crown of 48 in. HDPE pipes was reduced by 2 to 3 times as compared to the 36 in. HDPE pipes. AASHTO design deflection limit of 5% was found to be suitable for installation with shallow cover. Since the soil was compacted to a minimum of 95% of standard proctor maximum density, the pipe had adequate support around it. This was demonstrated by the fact that the soil pressure at the haunch and invert regions were only 15-35% of the pressure at the crown.

Bayoglu Flener (2009) performed static load tests on four corrugated steel box culverts with 46- and 26-ft spans (two of each) under varying cover thickness. One culvert of each span was stiffened at the crown. The load was applied using fully loaded truck with weight of 48 psi and 35 psi for 26- and 46-ft span respectively. The effect of depth of cover on the culvert was not linear with the culvert becoming more vulnerable at decreasing cover depths. The application of crown stiffening proved to be an effective mechanism to reduce tension at the bottom of the section. The stiffening also proved to more effective under shallow cover with the difference in maximum displacement between the stiffened and unstiffened culvert at shallow cover being approximately twice.

Moore and Garcia (2015) performed several laboratory tests on 40 in. diameter deteriorated corrugated steel culverts, buried under a 4 ft. soil cover and rehabilitated using sprayed-on cementitious liners. The pipes had a corrugation profile of 2-2/3 in. by 1/2 in. and were between 0.071-0.075in. thick prior to any corrosion. The loads on the culvert were applied from the surface using single axle load and tandem axle load. A thickness survey performed on the deteriorated pipes showed that the damage to the culvert was limited to the invert region i.e., the area between the two haunches. The reduction in wall thickness along the invert was between 0.051 to 0.063 in., with perforation seen in some locations. These deteriorated pipes were first tested under single axle load of 30 psi to establish a base line and stabilize the system prior to lining. Even at this deteriorated state, the pipes showed no sign of failure and were deemed sufficiently stable for the examined configuration. However, since the purpose of the tests were to evaluate the capacity of the sprayed-on cementitious liner, the deteriorated culverts were not loaded beyond 30 psi and hence their ultimate capacity remained unknown.

Mai et al. (2013) studied the impact of corrosion and the resulting reduced wall thickness on the strength of corrugated metal culverts using numerical modeling as well as full scale testing. The two tested culverts both showed corrosion along the invert with one culvert more deteriorated than the other. The heavily corroded culvert had about 30 to 52% of the original wall thickness corroded between the haunches while the lightly corroded culvert had about 10 to 17% corroded. The walls of both the culverts were intact and free of perforations. Van Thein also varied the quality of backfill with a well-compacted backfill (92%) on the lightly corroded culvert and loosely compacted backfill (86%) on the more deteriorated culvert. The load was applied using single axle as well as single wheel pair. The load was applied for two different cover depths (3 ft and 2 ft). As seen in previous studies, the culvert showed more critical response under shallower cover. It was also seen that the heavily deteriorated culvert with loose backfill deformed more as compared to the lightly corroded culvert. At failure, buckling was seen in steel surrounding the perforated areas of the culvert while a plastic hinge formed at the crown. However, even though the heavily deteriorated culvert was weaker, it was still able to carry the single axle working load and did not fail up to 49 psi which was equal to 90% of the fully factored single axle load based on both AASHTO and Canadian design truck

loads. This observation lead to the conclusion that even deteriorated metal culverts may be able to carry significant load.

Sargand et al. (2018) studied the load capacity of corrugated steel pipe arch with extreme corrosion under shallow cover on real field conditions. The behavior of a corroded section of the culvert was compared to the behavior of the section repaired using concrete paving at the invert under external loads of up to 60 kips. While the invert paving certainly improved the culvert performance, even the corroded section of the culvert was seen to have significant load-carrying capacity remaining with the plastic limit of the steel exceeding at a value higher than three times the legal load limit.

Masada (2017) compared the behavior of culverts with extreme invert deterioration with the same repaired using concrete paving of invert. The in-service CMP had 102 in. diameter while the in-service arch had 83 in. rise by 123 in. span. Service load tests were conducted on both of these pipes as they were due for repair on field. Additionally, ultimate load tests were conducted on new pipes with artificially perforated inverts. Both sets of pipes were then repaired using invert paving and retested. It was observed that during the ultimate load test of artificially perforated pipes, the earth pressures dropped, and the soil fill over the pipe settled more. The structure was also seen to deflect more in the horizontal direction than when the invert was intact. The backfill material was found to have pushed into the pipe through the perforations, further weakening the soil support. The ultimate load capacity of the artificially perforated pipe was found to be reduced by 73% as compared to the intact pipe. At failure, seam splitting and excessive deflections were observed in the damaged pipe. While the deteriorated pipes were certainly weaker than the intact and repaired samples, they were still able to handle the service loads. For the field installations, service load test on the pipe prior to and after invert paving showed a 40% reduction in vertical deflection and about 12% reduction in horizontal deflection. This study further improved upon the capacity of CMPs with significantly deteriorated invert.

2.6 Past Studies Using Finite Element Modeling

Performing full-scale tests on pipe soil systems is a significant undertaking. The amount of time, effort and cost it takes makes performing multiple full-scale tests to study the influence of various factors unfeasible in most of the research studies. Furthermore, in absence of proper literature, designing a suitable experiment plan for such studies is also complicated. Hence, use of finite element modeling has been used over the years to better evaluate the design equations and perform numerous studies into the behavior of a pipe-soil system.

Moore and Brachman (1994) performed a theoretical three-dimensional modeling to model the performance of buried circular culverts, buried under shallow cover and subjected to vehicle live loads. Due to limited computing power of the time, Moore and Brachman used various simplifications to theoretically model the applied live load and the

system's response to it. The model was found to be an improvement over the two-dimensional finite element calculations and provided better predictions of hoop-thrust distribution.

Girges and Abdel-Sayed (1995) performed 3D finite element modeling of a theoretical steel culvert buried in soil to study the 3D interaction between the pipe and soil when the dead load due to soil cover varies in the longitudinal direction. The results from the 3D model were compared to the predicted behavior form classical 2D models and prevalent design codes. The 3D model was found to better predict the soil pressure distribution than that by the AASHTO codes. However, the magnitude of thrusts predicted were similar to that predicted by the 2D model. The 3D model also showed 10% higher buckling load as compared to the 2D model.

Crosby (2003) performed 2D and 3D finite element (FE) analyses of a soil box testing facility developed for testing the structural response of buried fiber reinforced and standard reinforced concrete pipes using Plaxis. The results of 3D analyses were used to verify the 2D analyses. Various factors like the influence of interface friction angle, to study the pipe-soil interaction, effective mean stresses along the sidewalls of the soil box to study the boundary effect, etc. were studied. However, due to lack of experimental verification, this was more of a theoretical exercise.

Mai et al. (2018) performed a similar study as Crosby in that they utilized finite element analysis to evaluate the maximum size of pipes that can be tested in their test facility. Both 2D and 3D models were used to assess the impact of top, side and bottom boundaries for both flexible and rigid pipes with varying diameters. In addition, use of two steel grillages to provide a uniform overburden pressure over the soil was also examined. Effect of friction due to proximity to sidewall and height of pipe form the concrete floor were also considered to observe the system response. However, this was a preliminary study performed to make an informed decision about the size of pipes to be tested, possible test setups and loading mechanisms and thus lacked experimental verifications.

El-Sawy (2003) performed 3D FE analyses of two functioning corrugated metal pipes (CMPs) and compared the model performance with the experimental results. The field culverts had varying overburden with exposed ends. The 3D FE models were created using both the actual filed overburden and a simplified geometry with constant overburden. The soil and culvert materials were both considered to behave elastically and hence couldn't be used to model behavior under extreme cases. The corrugated geometry of the culvert was simplified to a plane plate model by modifying the thickness and elastic modulus such that the axial and bending stiffness remained the same. Two types of equivalent plane plates were considered: isotropic plane plate and orthotropic plane plate. The study concluded that the soil modulus had a generally smaller effect on the circumferential thrusts in orthotropic model as compared to isotropic model. The orthotropic model had better match with the experimental values as compared to the isotropic model. For both models, it was also seen that the circumferential thrust decayed

within a short distance and hence could be modeled using a simplified geometry with long prismatic soil geometry (constant overburden). The thrusts obtained from 3D models were within 30% of the measure ones. The main limitation to this study was the linear elastic assumption used for modeling both the soil and the CMP.

El-Taher and Moore (2008) used 2D finite element analysis to study the residual capacities of deteriorated CMPs. The study was purely theoretical in that it lacked experimental comparisons. However, it did present a general idea for behavior of deteriorated culverts. It further simplified the problem by assuming the system behavior to be linear elastic. The effect of corrugated geometry was included in the 2D model by using a plane pipe with equivalent thickness and elastic modulus. The effect of deterioration due to corrosion was then modeled by reducing the wall thickness along the invert. The model performance was then studied for different cover thickness and pipe diameter. Due to the huge role that soil plays in the stability of pipe-soil systems, the change in thrust and moments due to corrosion of the invert were found to be negligible. Instead, it was the yielding of the pipe material that presented the critical limit. The model however couldn't account for the cases where the invert is perforated.

Mai et al. (2014) performed a study on the capability of 2D models to represent the behavior of deteriorated culverts by comparing the results obtained from two FE programs (Abaqus and CANDE) and calculations performed using American and Canadian design codes with experimental tests on two deteriorated culverts. Among the experimental specimen, one culvert was highly deteriorated and buried under loose/poor quality backfill while the second specimen was lightly corroded and buried under well compacted/good quality backfill soil. The corrugated culvert geometry was converted to equivalent plane plate using similar approach as used in previous studies. The analyses performed using 2D models were found to provide conservative predictions for thrust forces while the forces obtained using Canadian (CHBDC) and American (AASHTO) design codes were found to be unconservative. However, since the system was assumed to be linear elastic for all analyses, none of the models could capture the non-linear behavior observed during the later stages of the experimental tests.

Campbell (2018) performed 3D FE modeling to improve on previous 2D model representing corroded culvert performance. The model first modeled an intact 3D culvert and compared the results with the experimental results used by Mai (2013)This study included a major improvement on the previous studies in that additional models were prepared to represent non-linear soil behavior and compare it with linear elastic model. The model's performance was also compared with previous 2D models. Further parametric studies were conducted to study the influence of various input parameters on capacities of intact and corroded CMPs. A wide range of input parameters including pipe diameter, cover thickness, soil stiffness, soil strength and soil-pipe interaction were studied for intact CMPs. The models showed that pipe diameter and cover thickness had the highest impact on total forces induced in the CMPs. Furthermore, corrosion geometry and remaining plate thickness were used as varying input to study the influence of

corrosion. Corrosion was found to have a significant effect in reducing the factor of safety of the CMPs against yielding and buckling with the most critical location for corrosion located at the haunches. The non-linear soil models performed significantly better that the linear elastic model. The extent of corrosion was found to be minor impact on the total forces on the CMP. On the other hand, the factor of safety against yielding decreased linearly and the maximum normal stress increased exponentially with decreasing plate thickness. Similar to previous studies, this study too used an orthotropic equivalent plane plate model to represent the corrugated geometry of the CMP.

Elshimi (2011) performed 3D FE analysis with explicit modeling of a corrugated box culvert, which was then compared with the performance of a 2D and orthotropic plane pipe model. The results from all models were also compared with experimental data from laboratory tests. The 2D model successfully calculated the deformed shape of the box culvert and was able to obtain similar bending moments as obtained from the experiment. However, it neglected the low stiffness of the culvert in axial direction. This deficiency was covered by both the orthotropic and corrugated models. As a result, the 2D analysis overestimated the bending moment, especially at the shoulder. The corrugated model was found to provide an all-round better representation of the box culvert behavior at ultimate state conditions. An almost linear behavior was observed between bending moment and height of soil cover.

2.7 Summary

Corrugated metal culverts (CMPs) are an integral part of this nation's infrastructure. Being flexible in nature, these pipes are expected to deflect under load. CMPs derive a significant portion of their strength and stability through the support provided by the surrounding soil. While there are standards in place for design of CMPs, its repair is still being diligently studied by many researchers. Therefore, it is a good idea to have an idea about the kinds of damages and the resulting loss in strength and stability it causes to come up with effective and economic repair and rehabilitation protocols. The majority of past studies into deteriorated CMPs have shown that the most common damage to these systems is the loss of invert due to extreme corrosion and abrasion. While the majority of these studies have only loaded such deteriorated culverts to service load, there have also been a few studies that loaded them to failure. However, in each of these cases, the deteriorated pipe/culvert had some portions of its invert intact.

Out of the many finite element analyses conducted on the behavior of buried culverts, there are very few that have actually used the actual corrugated geometry of the culvert along with non-linear material properties and none (to the author's knowledge) that have used the actual geometry of the culvert to study invert loss. Therefore, it is unclear what contribution the intact portions of the CMP may have on the system's stability and failure mode. Therefore, as a simulation of the worst-case scenario, this study was concerned about the performance of a buried culvert with no invert whatsoever. It is hoped that this study will further supplement the information on the loss of strength

and stability of a pipe-soil system subjected to extreme levels of corrosion, thereby proving to be a valuable decision-making tool when inspecting need for repairs in field culverts or, while determining strength criteria to be met by suggested rehabilitation approaches.

Chapter 3 SOIL BOX TESTS

3.1Test Setup

A full-scale laboratory test on buried CMPs was designed for the soil box at CUIRE. The soil box is 25 feet long, 12 feet wide and 10 feet height. This is divided into three cells along the length using wooden partition walls, with each cell being 6 feet long. A hydraulic actuator is installed to apply the load. A reaction frame is installed inside the soil box to support the actuator. The load from the actuator was applied to the soil using a steel load pad of dimension 10 in. by 20 in. This load pad was chosen to represent the standard contact area from the wheels of an AASHTO H20 truck. The two end cells held two circular CMPs (intact and removable invert) while, the middle cell held a corrugated metal arch. The cells were each tested one at a time. Only the tests and results obtained from the circular CMPs are within the scope of this thesis.

Figure 3-1: Soil box before (left) and after (right) installation of the CMPS (source: CUIRE Laboratory)

3.2 Embedment and Backfill Soil

During field installation, in either trench or embankment conditions, different soil types are used as foundation/bedding and backfill materials according to the type/quality of installation. For the purpose of this study, type 3 installation has been chosen to stay on the conservative side when it comes to field applications. Type 3 installation allows the use of either sandy/gravelly soil (compacted to a minimum of 85% of maximum dry density obtained through standard proctor compaction test) or silty soil (90% compaction) or clayey soil (95% compaction) (AASHTO 2002). To achieve higher degree of control over the soil conditions and properties in a short time, granular soil was chosen to be used in

this study. Variation in moisture content can play a significant role in determining the maximum dry density for clayey and silty soils. However, in cases of free draining soils like sand and gravel, the moisture content has relatively low effect on the variation in density. Past studies into the behavior of such soils has shown that the maximum dry density for these soils is observed either in dry state of near saturated state (Bergeson et al. 1998; Drnevich and Evans 2007; USBR 1998). The reason behind this behavior in free draining, cohesionless soils is the phenomenon called bulking. The capillary stresses developed in the soil at low water contents that cause bulking also contribute to resisting the compactive effort and, hence preventing effective compaction. This low-dependence on moisture content would allow for easier storage and use of the soil during the laboratory tests. Hence, granular soils were identified as the best fit for this study.

Two different types of soils have been used in this test. First, foundation, bedding and embedment to the CMP is provided using concrete sand. This is then backfilled by a layer of gravel. Concrete sand is a tan to light brown coarse sand that has been washed and screened to have larger particle size than common masonry sand. It is used in various applications like preparing ready-mix course concrete, pipe bedding, installation of paving stones, etc. Hanson pipes and precast were willing to support the study and provided the required concrete sand. The required amount gravel was obtained from the stored pile at UTA. Several laboratory tests, described in the following sections, were then conducted on the samples to classify and characterize the sand.

3.2.1 Sieve Analysis

Sieve analysis was performed on the samples of concrete sand and gravel to classify them according to the Unified Soil Classification System (USCS). Grain size distribution curve for both soils is provided in Figure 3-2. Concrete sand was classified as Poorly Graded Sand (SP) while the gravel was classified as Poorly Graded Gravel with Sand (GP). For both types of soils, the percentage of fine particles was less than 1%.

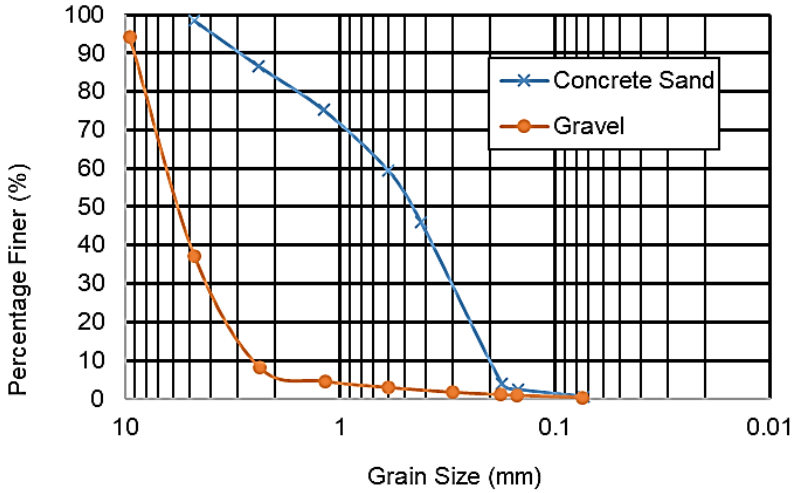

Figure 3-2: Grain size distribution curve for concrete sand and gravel

3.2.2Standard Proctor Compaction Test

Standard proctor compaction test was performed to check for the maximum dry density and moisture behavior of the soil. The maximum dry density of the sand was found to be 115.2 pcf at zero percent moisture content (oven dried condition). The in-situ moisture content was found to be approximately 6%. For moisture content variation from zero to twelve percent, the dry density variation was within 5 pcf (approx.). For the gravel, the amount of moisture it could keep was not very significant and during compaction, water was seen to be leaking out of the proctor mold even at low water contents. As a result, the moisture-density curve obtained was very uneven and did not provide useful data. This further verifies that moisture content plays a fairly small role when determining the density for granular, free-draining soils.

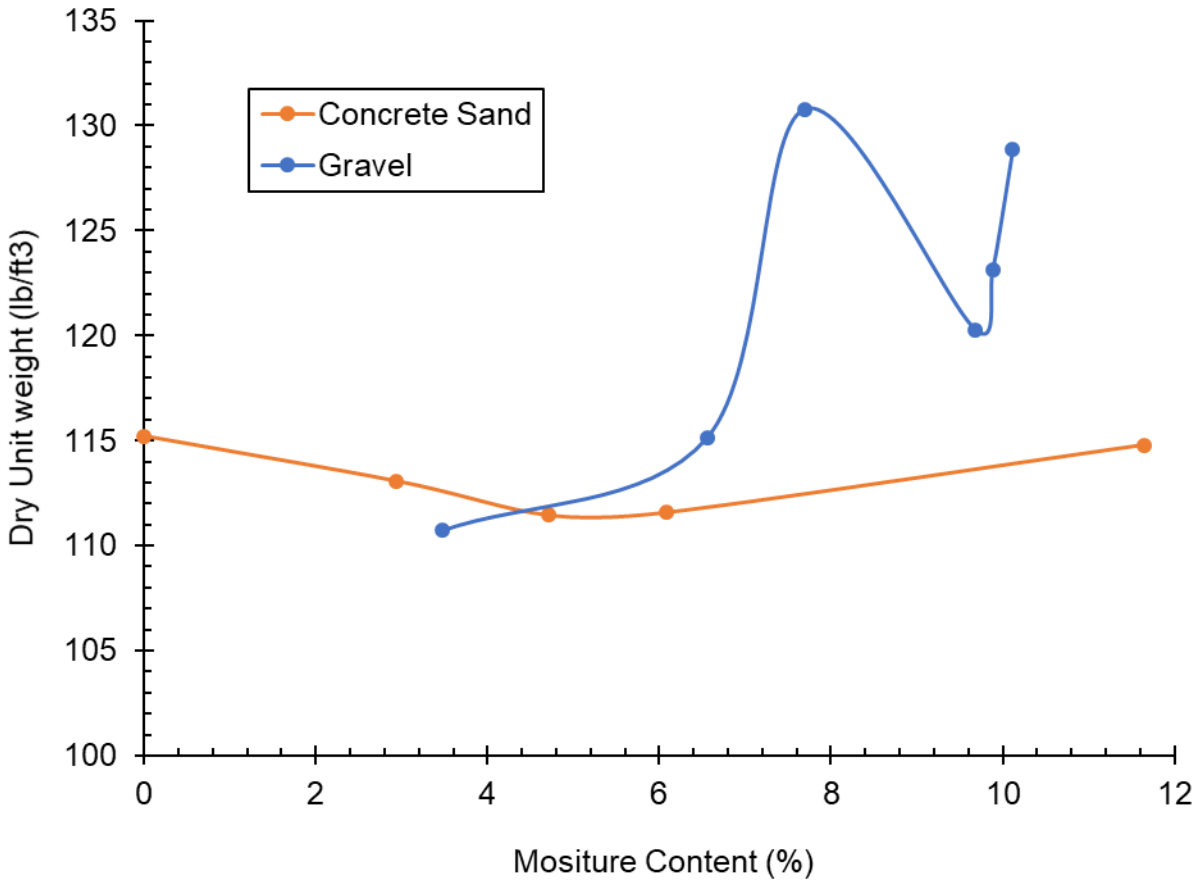

Figure 3-3: Moisture-density curve for sand and gravel.

3.3 Specimen Details

The CMPs used in this study were obtained courtesy of Contech Engineered Solutions. Two types of CMPs were obtained from Contech: one was a regular intact CMP with annular corrugations and other was a custom-made CMP with removable invert. Each of the CMPs were 6 ft. long with 60 in. diameter and had a corrugation profile of 2-2/3 in. by 1-2 in. The CMPs had a wall thickness of 0.109 inches.

Figure 3-4: Regular CMP (left) and CMP with removable invert (right).
(source: CUIRE Laboratory)

3.4Burial Configuration

The CMPs were buried under a sandy backfill soil. A 24 in. foundation was provided beneath the CMP to raise the height of the setup close to the ground level. The foundation was compacted using two passes of a vibratory plate compactor to obtain compaction level higher than 90% of standard proctor maximum dry density. Middle one third of the top 4 in. of foundation was disturbed to provide a suitable bedding for the CMP. For embedment, the sand was directly dumped into the soil box and levelled in lifts of 8 inches. Density measurement was taken at four locations for each lift using nuclear density gauge. An average compaction of 85% was obtained in the embedment by just dumping the sand. The sand layer was extended to 1 ft. over the top of the CMP. After which, a 1 ft. thick layer of gravel was placed over it to act as a pavement layer. The top gravel layer provided an additional function of delaying the bearing capacity failure of the soil when loading. Figure 3-5 shows the burial configuration during the test setup.

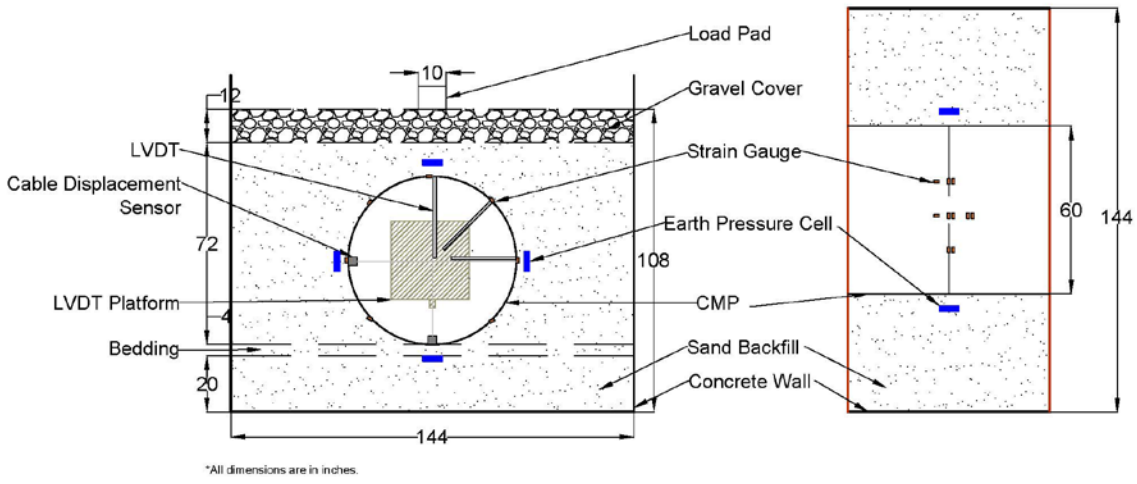

Figure 3-5: CMP test setup: cross-section (left) and plan (right) view.

3.5 Instrumentation

The CMPs were extensively instrumented to monitor the system response during loading. The instrumented section was directly below the centerline of the load pad on the surface as this was considered the most critical section under this loading condition. Strain gauges from Micro Measurements, model C2A-06-250LW-120 were used to measure strains at different locations in both the CMPs. Two layers of strain gauges were installed on crest and valley of the CMPs at eight locations along the hoop direction at 45° intervals, except at the invert. Since one of the CMPs would have no invert during testing, instrumenting this section was deemed redundant. One longitudinal strain gauge was installed at crown and east springline to monitor the longitudinal behavior of the CMPs. An additional layer of strain gauges was installed at crown level, one corrugation away from the center, to obtain additional information and act as a backup should the other layer of gauge malfunction. After installation, each strain gauge was provided with an acrylic coating to protect against moisture and chemical disturbance. A layer of aluminum foil tape was then added over each of the gauges to provide mechanical protection. Finally, all the gauges and their wires along the pipe circumference were covered with duct tape and brought out through a PVC pipe installed against the concrete sidewall. The data from the strain gauges was then obtained using the Model 7000 data acquisition system from Micro Measurements.

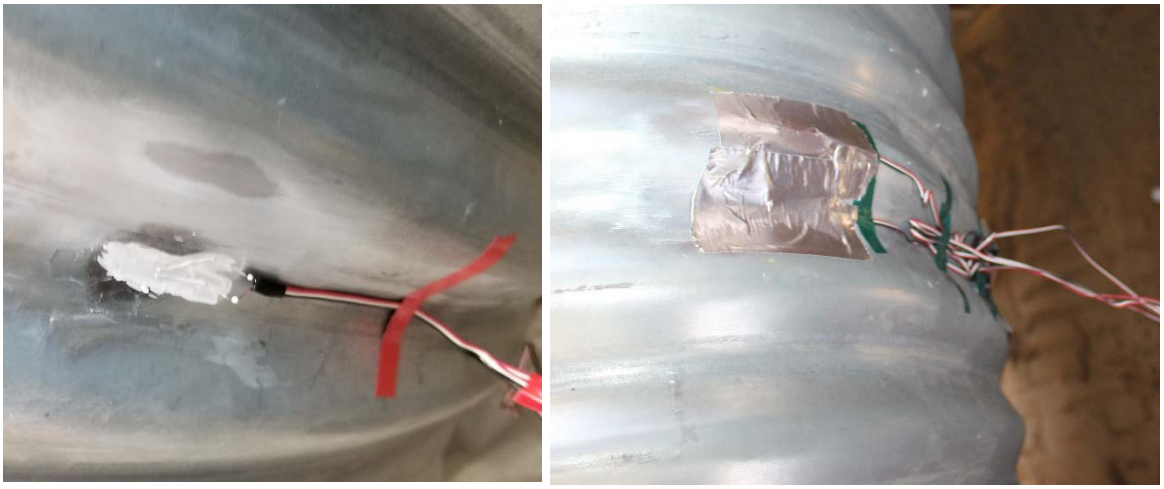

Figure 3-6: Acrylic coating (left) and aluminum foil tape (right) over the gauge. (source: CUIRE Laboratory)

Figure 3-7: Wiring and final duct tape covering over the strain gauges.
(source: CUIRE Laboratory)

Cable displacement sensors from Micro Epsilon, model WPS-500-MK30, and high accuracy displacement transducers (LVDT), model LD620-150 were used to measure the pipe deflection. Three cameras were also installed to observe the test progress. An instrumentation platform was made to install the displacement sensors and cameras inside the CMPs (Figure 3-8). An AC to DC battery was used to provide excitation voltage for both LD620 and WPS-500. The data from both types of sensors were recorded using midi logger GL 820 from Graphtec.

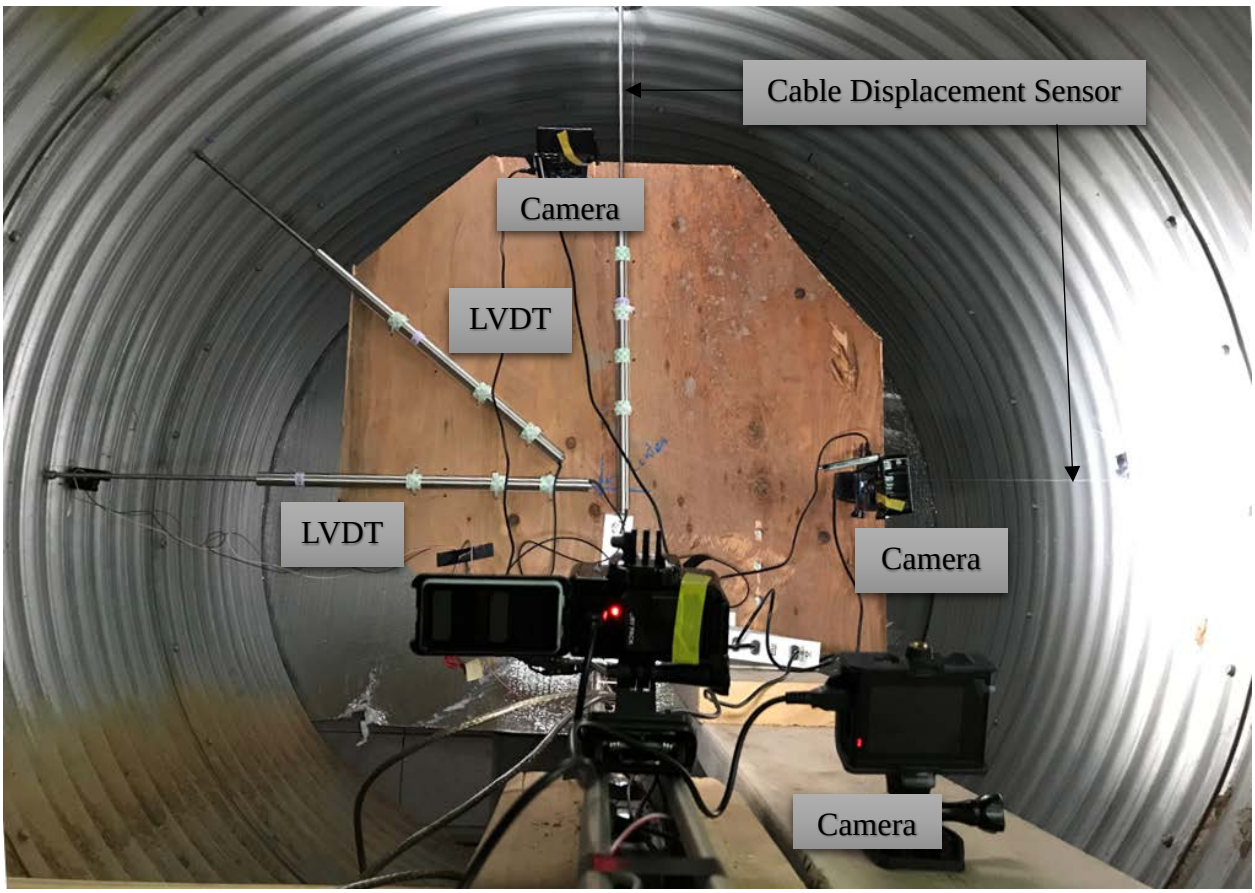

Figure 3-8: Installed displacement sensors and cameras.
(source: CUIRE Laboratory)

The soil pressure around the pipe was monitored using earth pressure cells from Geokon, model 4815-350kPa. The cells were placed at invert and crown levels to measure vertical soil pressure and at springlines to measure horizontal soil pressure (Figure 3-5). At each location, the cells were placed four inches away from the pipe surface to provide uniform contact area. The output from the earth pressure cells was read using vibrating wire data logger (LC-2 series, model 8002-16) from Geokon.

3.6 Load Rate

A finite rate of loading needs to be chosen for performing the soil box test. A culvert buried in field conditions faces dead loads from the weight of the soil column and live loads due to the vehicles moving over the pavement. While the loads due to the vehicles are usually dynamic in nature, AASHTO LRFD Bridge Design Specifications has included various factors to convert this load into an equivalent static load (AASHTO 2017). This factored load then shall be considered as the service load limit for the culvert during static testing.

There are generally two criteria that govern the application of load, viz. load/force criteria and displacement criteria. The load criteria also called the load/force-controlled loading monitors the load that is being applied to the system. In this situation, the stopping condition for the test is met when a certain value of load is reached. This method is often used in geotechnical load test, such as pile load tests, to determine failure load. It is a useful control mechanism when a system is to be loaded to a certain predefined load limit. However, in cases where the post peak behavior of the system is of interest, this criterion becomes unsuitable as once the peak is crossed, the load drops and the system will have two values of displacements for a single load. Therefore, if load control criterion is used in these cases, the test is terminated before the peak value is reached. Displacement control, on the other hand, monitors the displacement that is being caused due to the applied load. Since displacement in a system always keeps on increasing as long as the load is applied, this allows for monitoring the post peak behavior of a system. Since the purpose of this study is to obtain the ultimate load capacity curve for the culvert with no invert, the post peak behavior of the system is of great interest. Hence, displacement-controlled loading is deemed more suitable for this study. However, a finite number for the load still needs to be determined.

According to ASTM C497, for three-edge bearing test (D-Load test) of reinforced concrete pipes, any load rate up to a maximum of 7500lbf/linear foot of pipe per minute can used for up to 75% of the design strength after which, the rate is then reduced to a maximum of 1/3 of the design strength (ASTM 2019). However, this load rate is for the testing of a rigid pipe alone and its applicability during testing of a pipe-soil system is suspect. ASTM D2412 specifies procedure for parallel plate loading of plastic pipes. According to the standard, the load for this test is applied at a constant rate of 0.5 in/min(ASTM 2008). While this test is used for what is basically a flexible pipe, it still only monitors the behavior of a standalone pipe and hence is not concerned with the change in load pattern due to pipe-soil interaction. According to ASTM D1633, for determining the compressive strength of molded soil-cement cylinders, the recommended load rate is 0.05 in./min (ASTM 2017). Similarly, according to ASTM D2850, the load rate for unconsolidated undrained triaxial compression test of cohesive soils is 1%/min which, for a standard specimen size, comes to be approximately 0.025 in./min (ASTM 2015). However, similar to previous standards, these standards too cannot be used to account for the load interaction due to pipe-soil interface.

Howard (1972) performed laboratory load test on buried flexible pipe. The loads were applied in increments, at a rate of 2 psi/min, and held constant for one hour after each increment to allow for the time-dependent settlement (consolidation) of the clay backfill. Lougheed (2008) used a displacement-controlled method with a loading rate of 1 mm/min at 2 mm increment in a loading test of buried large-scale corrugated metal culvert. Becerril García and Moore (2015) performed soil box test on lined corrugated metal culverts, buried in granular soil. For the service load test of the culverts, the load was applied in two cycles with each cycle continuing to the full-service load. The first was

applied as a single increment to settle the system while the second cycle was applied in increments of 20% or 25%. To test the ultimate load of the culverts, the service load was applied in three load increments after which, a smaller increment (11.2 kips) was chosen until the maximum load was obtained. Regier, Hoult, and Moore (2016) tested a buried elliptical corrugated metal culvert for service and ultimate load using tandem axle configuration. The test specimen was loaded in three cycles for service load testing following which, it was loaded till failure to obtain the ultimate load. For all cases, a loading rate of 11.2 kips/min was adopted.

Besides the aforementioned tests, there have been several other tests that have tested the load capacity of different types of buried culverts under different situations. However, the one common theme among majority of these studies is that they generally do not provide the load rate used during the tests. Even in the papers (like the ones mentioned above) that do mention the load rate, there is no clear reasoning/justification behind the load rate adopted. Similarly, any of the existing standards (ASTM, AASHTO, etc.) do not have a standard testing procedure that can answer this question sufficiently. However, the concept that all the prior studies have accepted is that since the study of buried pipe entails loading a pipe-soil system where the load has to be transferred through the soil, a quick rate of loading is not suitable as it won't allow the time for soil to reach equilibrium and hence, for the system to stabilize. The appropriate loading rate should allow the testing soil (sand and gravel) to adjust its contact and rotation to balance the increasing stress and therefore, to eliminate the loading rate effect. Keeping this in mind, there are two possible ways through which load can be applied to a pipe-soil system. The load can be either be applied at a quick rate and held constant at predefined increments to allow the system to stabilize or, at a slow enough rate so that the soil has sufficient time to distribute the load as its being applied. This decision should be based on the type of soil and desire duration of testing. For granular soils like the type being used in this study, the time it takes for the soil to transfer the load and the system to stabilize especially at a shallow cover is a lot less than the time required for clayey soils. Hence, if continuous data recording is available, slow and continuous loading can provide a fair estimation of how the pipe-soil system would behave along with plenty of data points. However, since no concrete number for load rate was identified through literature search, a conservative value of 0.03 in. /min. is chosen for this study.

3.7 Test Procedure

First, the intact CMP was tested to obtain the baseline data. This was followed by testing of the CMP with removable invert. The testing of the CMP with removable invert followed the following sequence:

1. A 24 in. foundation layer of concrete sand was placed at the bottom. The foundation was placed in lifts of 8 in. and compacted using two passes of a vibratory plate compacter.

2. The middle one third of the top 4 in. of the foundation was disturbed to provide bedding for the CMPs.
3. An earth pressure cell, measuring vertical stress, was installed below the bottom of the pipe. The cell was placed 4 inches away from the CMP surface to provide proper backing.
4. The CMP was placed at the top of the bedding layer.
5. Strain gauges were installed on the CMP at the predefined locations.
6. Backfilling was started. The sand was dumped into the soil box and levelled to achieve 8 in. lifts. No additional compaction was done, and no effort was made to pack soil into the haunch areas. This represents cases of poor installation or cases where loss of invert and resulting seepage has disturbed the soil support.
7. Compaction was measured using nuclear density gauge after each lift at four locations around the CMP.
8. Two earth pressure cells measuring horizontal pressure were installed on either sides at the level of springline and one earth pressure cell measuring vertical pressure was installed at the top of the CMP. Each of the cells were installed 4 in. away from the CMP surface to provide proper backing.
9. Concrete sand was placed to a height of 1 ft. above the top of the CMP. An additional 1 ft. of gravel layer was added to the top.
10. After completion of backfill, the LVDT platform was installed inside the CMP and cable displacement sensor was setup to measure vertical displacement.
11. The invert of the CMP with removable invert was removed as the resulting crown movement was monitored using the cable displacement sensor.
12. LVDTs and cable displacement sensor to measure change in horizontal diameter were installed inside the CMP.
13. All the sensors were connected to their respective data acquisition systems.
14. Load was applied at a rate of 0.03 in./min. and the system response was monitored.

The test of the intact CMP followed the same sequence as the CMP with removable invert except for step 11. Instead, all the displacement sensors were installed at the same time and loading was started.

3.8 Results and Discussion

3.8.1 Test on Intact CMP

The first test was conducted on a sample of intact CMP. Load was applied using the hydraulic actuator at 0.03 in/min and the system response was monitored using the instrumentation discussed in previous section.

Load displacement behavior of cover soil

Initially, the load required to induce the prescribed displacement was high and a steep rise in load-displacement curve was seen as the top gravel layer started to resist the load (Figure 3-9). As the soil layers started to get to plastic state, the slope of the load-displacement curve started to reduce. At this state a peak load of approximately 21 kips was seen beyond which, the bearing failure of cover soil occurred, and the load was transferred directly to the pipe, leading to second increase in slope of the load-displacement plot and an eventual second peak in the curve.

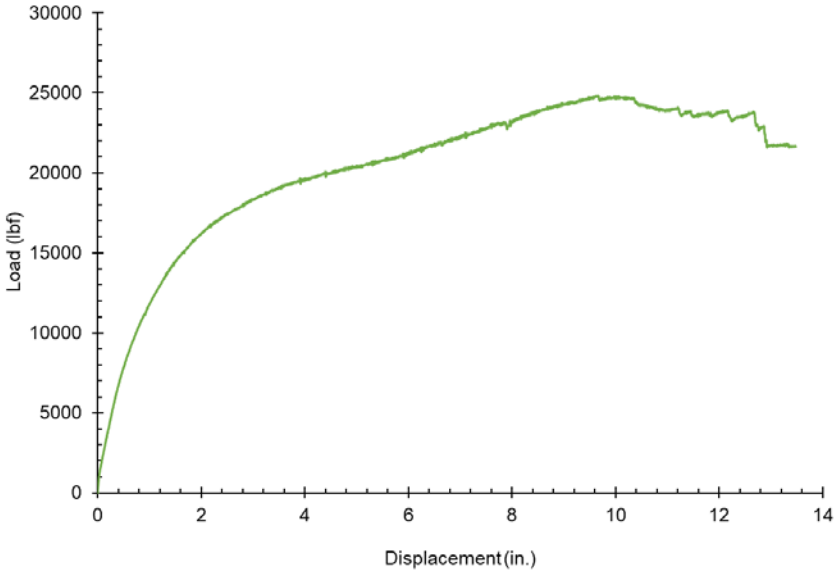

Figure 3-9: Load-displacement curve for the soil cover

After the test was completed, the soil below the load pad was examined. It was observed that most of the soil in the loaded area was the gravel used as top cover (Figure 3-10). This suggests that the upper rigid gravel layer punched through the weaker underlying sand layer during the test.

Figure 3-10: Bearing failure of soil below the load pad.
(source: CUIRE Laboratory)

Earth pressure distribution around the CMP

Earth pressure distribution around the CMP was monitored using the installed earth pressure cells. All the installed earth pressure cells had rated capacity of 51 psi. Highest earth pressure reading over the course of loading was seen at the earth pressure cell above the top of the pipe, along the line of the load pad. On the other hand, the earth pressure cells installed at the level of springline and invert showed very small readings of pressure. Since the values of the pressure shown were extremely low as compared to the rated capacity of the earth pressure cells, the accuracy of these numbers is suspect. However, they do hint that there was not significant load transferred to the sides of the CMP.

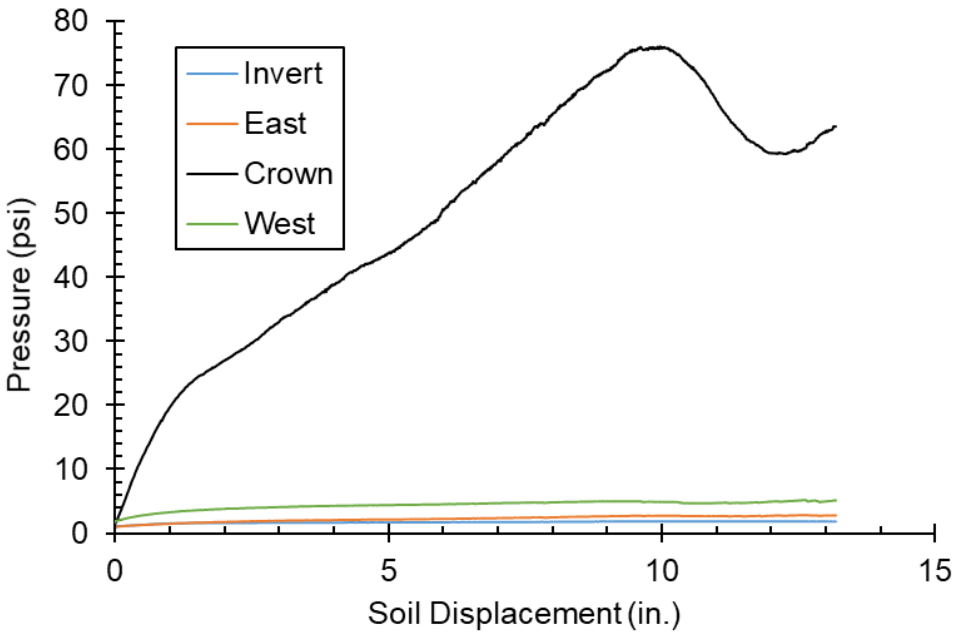

Figure 3-11: Earth pressure around the CMP.

Load displacement behavior of CMP

As the applied load was monitored by the actuator, simultaneous observation was made for the displacement of the pipe at crown, springline and east shoulder (Figure 3-12).

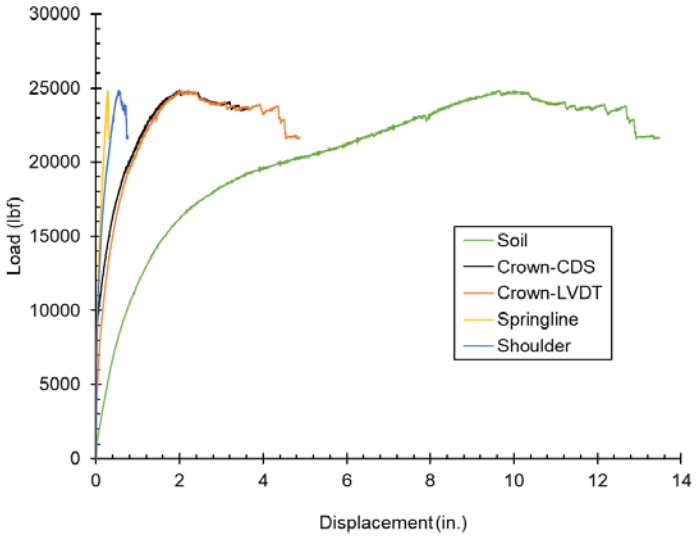

Figure 3-12: Load-displacement plots for soil and pipe

Initially, the displacement rate in the pipe was extremely slow, with rising displacement rate as the cover soil neared failure. The failure of the soil was highlighted by the corresponding increase in displacement rate of the pipe. As the CMP started taking

most of the load, the applied load kept on increasing and the ultimate load of approximately 25 kips was reached at the crown deflection of 2 inches (approx.). Beyond this point, the pipe started buckling and the load dropped. At the final state, the pipe had vertical crown deflection of 4.8 inches, which is higher than the 5% deflection limit set for flexible pipe. On the other hand, the springline of the CMP only had 0.3 inches of deflection. This incompatible deflection between the crown and springline suggests that the pipe failed in buckling. This observation was also validated by the pictures from the cameras installed inside the CMP (Figure 3-13).

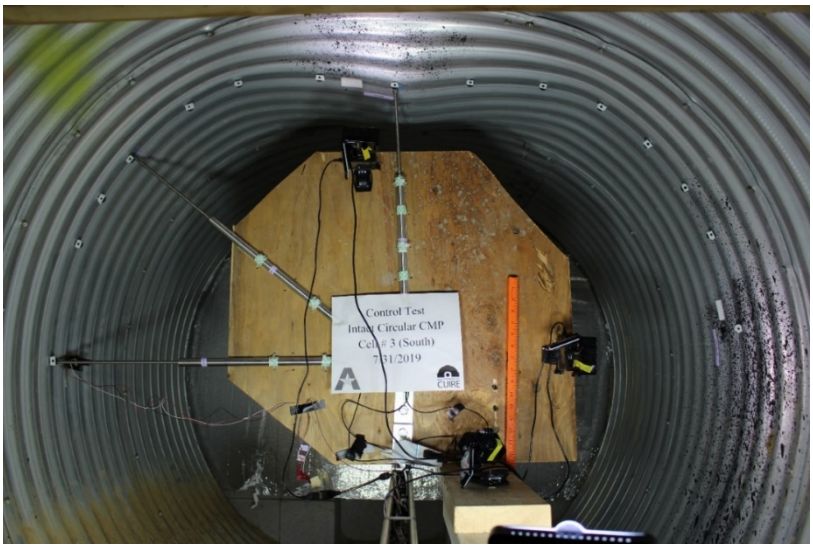

Figure 3-13: Localized buckling at pipe crown.
(source: CUIRE Laboratory)

Strains, Moments and Thrust

The strain gauges installed around CMP were monitored to observe the strain at different locations. The nomenclature used for the strain gauges are presented in Table 3-1: Nomenclature used for strain gauges.

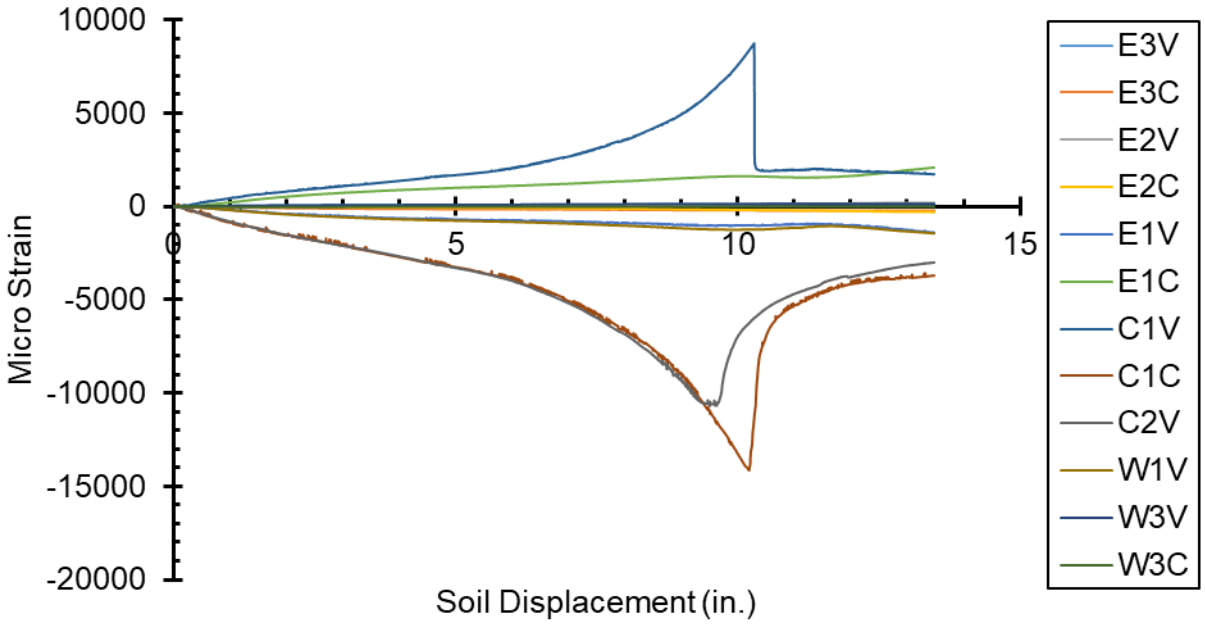

Figure 3-14: Strain at different locations during the test.

Table 3-1: Nomenclature used for strain gauges.

Location	Layer	Designation
East haunch	Crest	E3-C
	Valley	E3-V
East springline	Crest	E2-C
	Valley	E2-V
East shoulder	Crest	E1-C
	Valley	E1-V
Crown	Crest	C1-C
	Valley	C1-V
Crown offset	Crest	C2-C
	Valley	C2-V
West shoulder	Crest	W1-C
	Valley	W1-V
West springline	Crest	W2-C
	Valley	W2-V
West haunch	Crest	W3-C
	Valley	W3-V

The strains from corresponding crest and valley at each point were used to calculate the circumferential thrusts and bending moments at each location. Assuming linear distribution of strain, the circumferential bending moment and thrusts at different locations in the CMP were calculated by using the strain from crest and the corresponding valley as follows (Elshimi 2011):

$$M_\theta = \frac{EI_\theta(\varepsilon_{crest} - \varepsilon_{valley})}{d}$$

where:

M_θ= Circumferential bending moment (lbf-in./in.),
I_θ= Moment of inertia per unit length in the circumferential direction (in.^{4}/in.),
ε_{crest}= circumferential strain measured at crest of the corrugation,
ε_{valley}= circumferential strain measured at valley of the corrugation,
d= depth of corrugation (in.), and,

$$N_\theta = \frac{EA_\theta(\varepsilon_{crest} + \varepsilon_{valley})}{2}$$

where:
N_θ= circumferential thrust (lbf/in.),
A_θ= cross-section area per unit length in the circumferential direction.

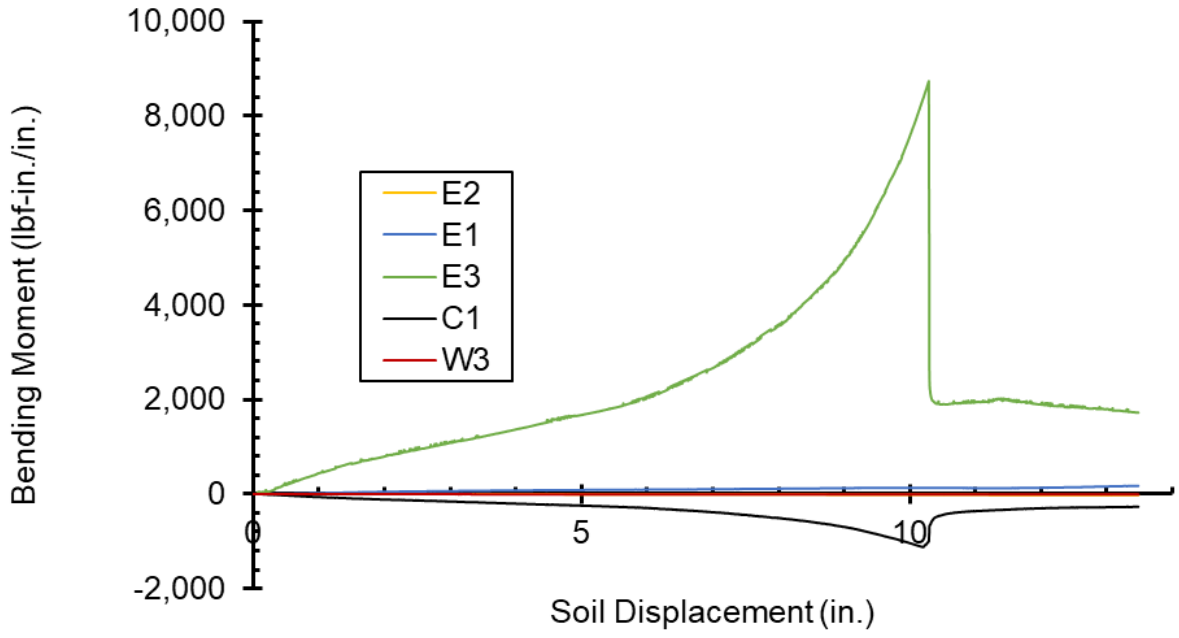

Figure 3-15: Variation of bending moment around the CMP during the test.

Maximum bending moment in the pipe was observed at the top of the pipe. The next high value for strain was located at the shoulder. The strain obtained from the gauges at haunch and springline levels were almost negligible compared to the readings from shoulder and crown. The strains at haunch, springline and shoulder kept rising as the test progressed however, the strain at the top dropped after the pipe started buckling.

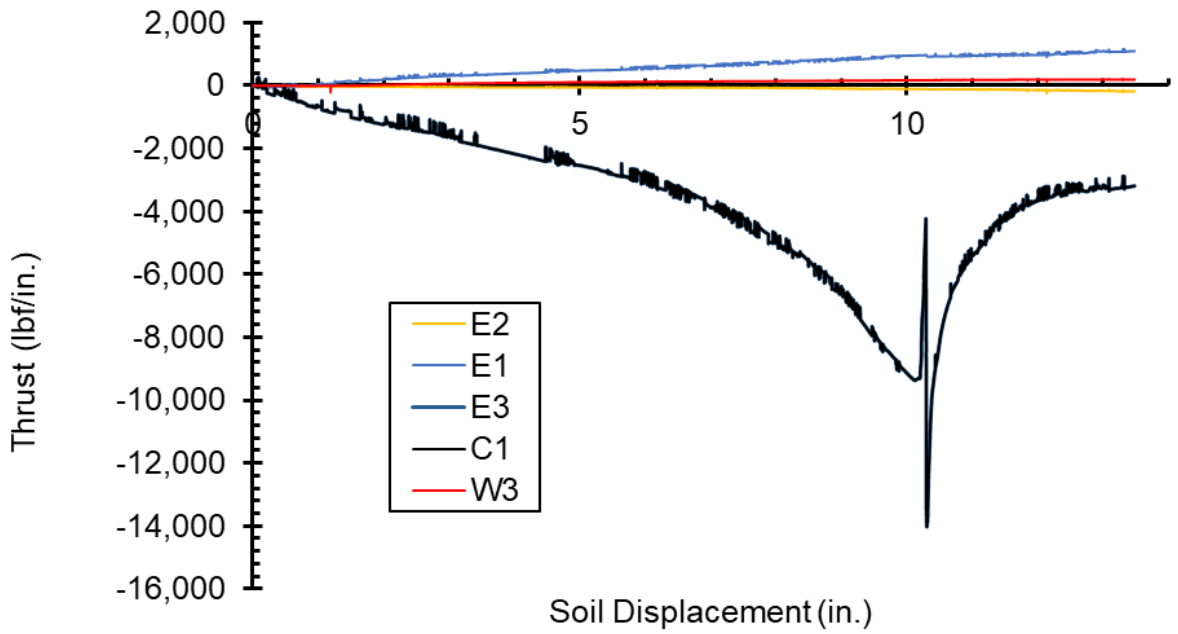

Figure 3-16: Variation of circumferential thrust around the CMP during the test.

The thrust distribution around the CMP followed the same pattern as the bending moment in that the maximum thrust was observed at the crown. Similar to bending moment, the thrust reduces as the CMP starts to buckle. The values of moments and thrusts at east and west sides of the CMP are fairly close i.e., the CMP behaves symmetrically about the YZ plane. This symmetricity is utilized in developing a more efficient model for finite element simulations of the test.

3.8.2 Test on Invert-Cut CMP

After completing the tests on intact CMP, a baseline data was obtained for the strength and capacity of the CMP. The next test was then conducted on the circular custom-made CMP with removable invert to study the effects of invert removal. Soil failure was observed in the intact CMP, which lead to local buckling and which is not a desirable failure mode. Therefore, to rectify the problem of soil failure during this test, the load at the soil surface was applied with a bigger load pad of size 20 in. by 40 in.

Before the application of external load, the invert of the CMP was removed. At this point, the CMP showed a heavy and sudden movement. The invert of cut edges of the CMP moved in by 9 inches and crown settled by 2 inches. This was accompanied by the similar settlement on the cover soil. The system stabilized once this initial movement was over. External load was then applied through the bigger load pad to begin the test. The results from this test are presented in the following sections.

Load displacement behavior

Figure 3-17 shows the combined load displacement plots obtained from the test for soil settlement and pipe deformation at crown, springline and shoulder.

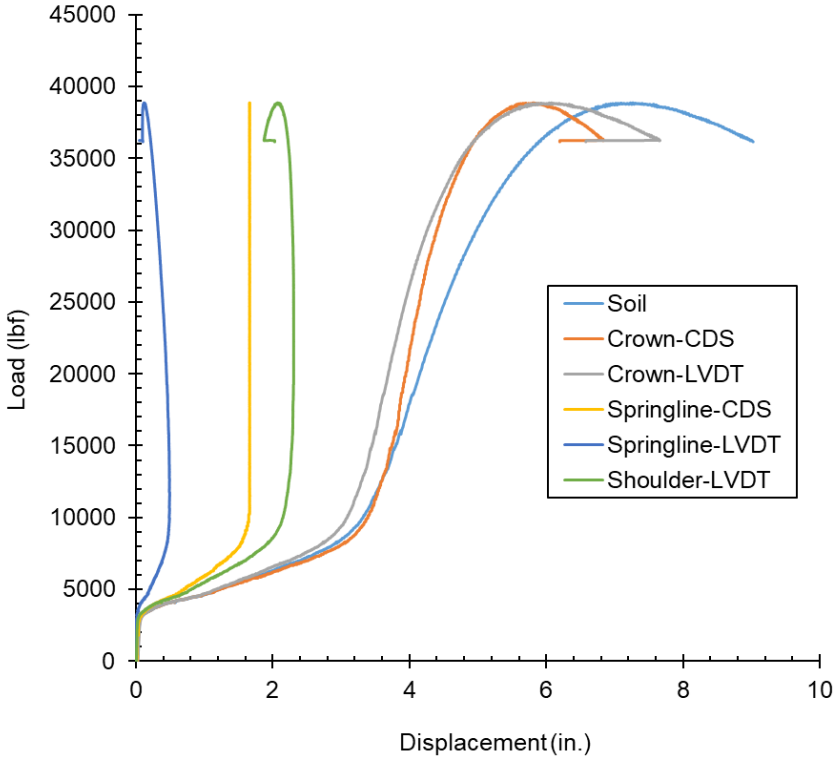

Figure 3-17: Combined load displacement plot for soil and pipe obtained from different sensors.

As load was applied to the soil, the load rises at a steep curve as the soil rearranges and presumably, closes the gaps formed due to the sudden movement when the invert of the CMP was removed. Once this is achieved, the slope of the curve begins to drop quite significantly. This drop is accompanied by settlement in the soil and increase in deflection in the pipe. Unlike intact CMP, the deflection at the crown and springline is significantly higher as the CMP has lost its ring stiffness and haunch area around the removed invert starts to move inward. This relatively easy deformation of the CMP is the reason the slope of the load-displacement curve has decreased. However, after a certain point, the system stiffens and the slope of the load-displacement curve increases. This is because the haunch area around the cut invert on either side have come in contact with each other and hence are providing a resisting force. The load taken by the system after this point is quite significant. However, since this is because a significant deflection has already occurred in the CMP before this point and the cut pieces have come in contact, this increase in strength is not useful and the CMP is considered to have failed at the point of slope increase. Hence, the completed curve was reduced to observe the system behavior prior to the cut edges coming in contact (Figure 3-18).

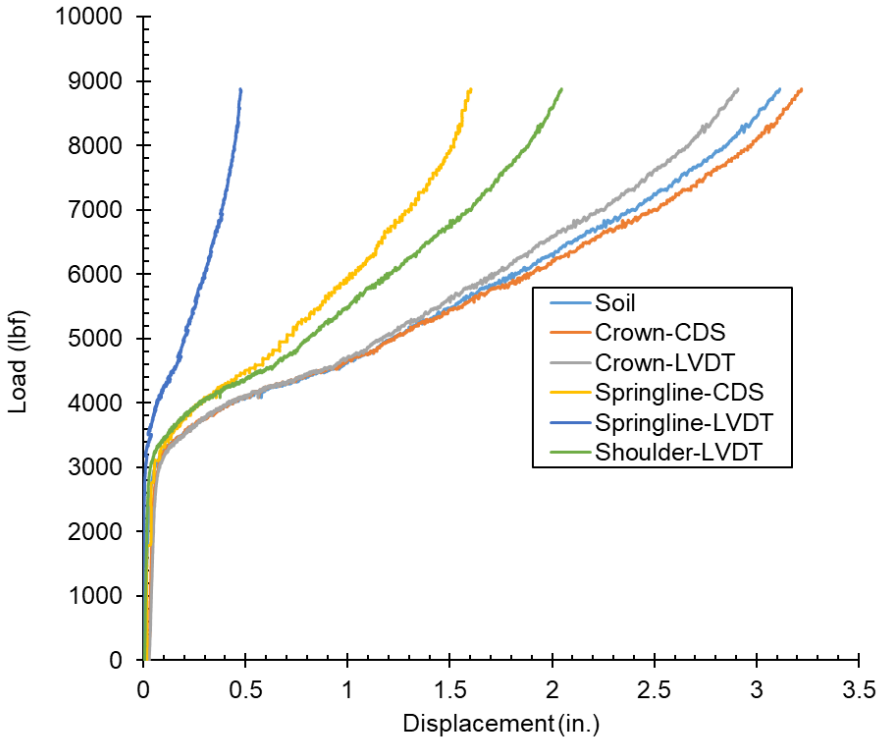

Figure 3-18: Shortened load displacement plots prior to cut edges coming in contact.

It can be observed that the load displacement plots for soil and pipe crown are almost co-incident towards the start of loading and continue to follow each other closely as the test progresses. This suggests that the settlement seen in the soil is purely due to the movement of the CMP as the cut edges of the invert move towards each other. As a result, the cover soil hasn't had to take significant load. Additionally, the side supports that could be provided by the backfill soil has been almost negligible as the springline of the CMP has moved inwards rather that outwards. The total soil settlement prior to the cut edges touching each other is approximately 3.5 inches, a lower value as compared to intact pipe. Hence, unlike the intact CMP, the limit/critical component of the soil-pipe system in this test is the invert-cut CMP.

Earth pressure distribution around the CMP

Figure 3-19 shows the earth pressure distribution around the CMP. Similar to intact CMP, the maximum earth pressure is observed at the crown though, the magnitude of the pressure is almost half of that observed during the test of intact CMP. Unlike intact CMP however, significant pressure is observed at the springline levels as well. Similar to the applied load, the pressure around the CMP also shows a significant increase once the cut edges of the invert meet (shown by the dashed line). The least pressure is observed at the invert level, which is as expected as there isn't an invert at all.

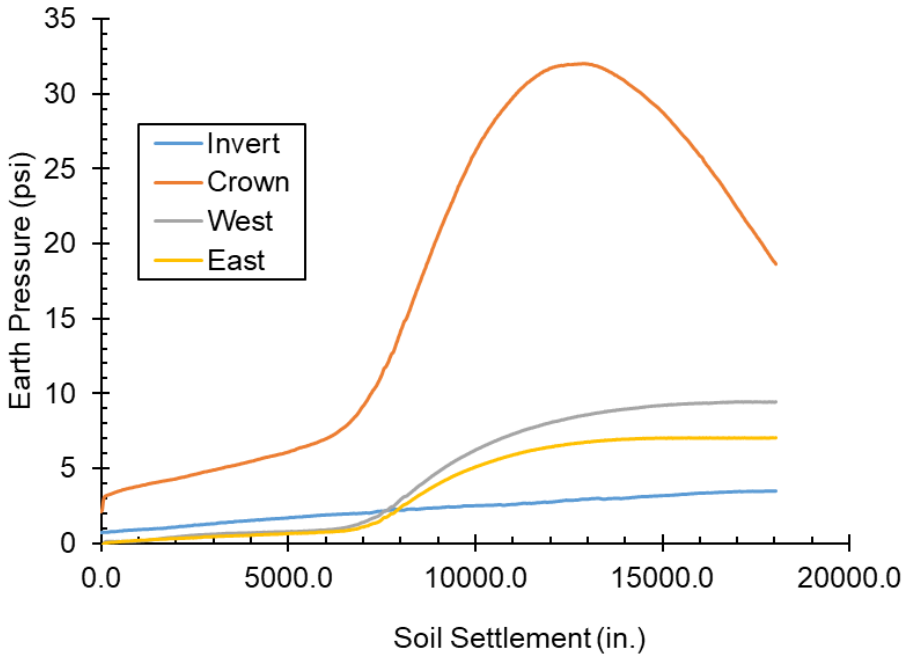

Figure 3-19: Earth pressure distribution around the CMP.

Strains, Moments and Thrusts

The strain gauges installed around the CMP were monitored to obtain the CMP's response to loading (Figure 3-20). However, a few of the gauges around the east side and crown of the CMP were found to have malfunctioned during the test. This might have happened due to sudden movement in the CMP as the invert was removed. Hence, the strains from these locations were excluded from any further analyses.

Circumferential bending moments (Figure 3-21) and thrusts (Figure 3-22) distribution were calculated using the same procedure used for intact CMP. It is immediately obvious that the thrust and moments at the locations away from the crown are much more significant than before. Since the moment and thrust information for the crown was not available, the maximum measured bending moment and thrust was observed at the shoulder location.

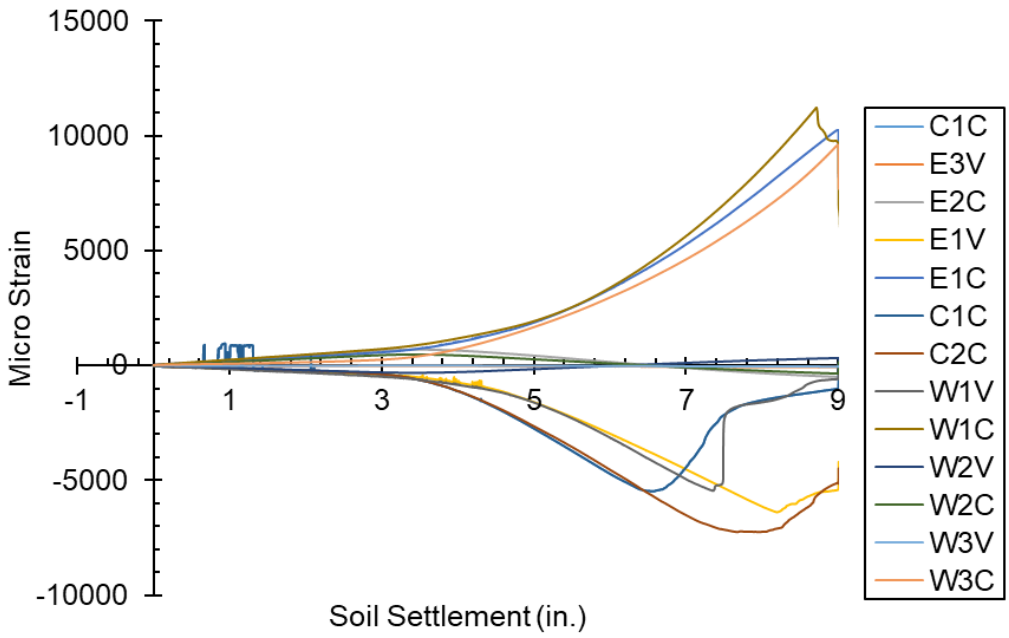

Figure 3-20: Strain distribution around the CMP.

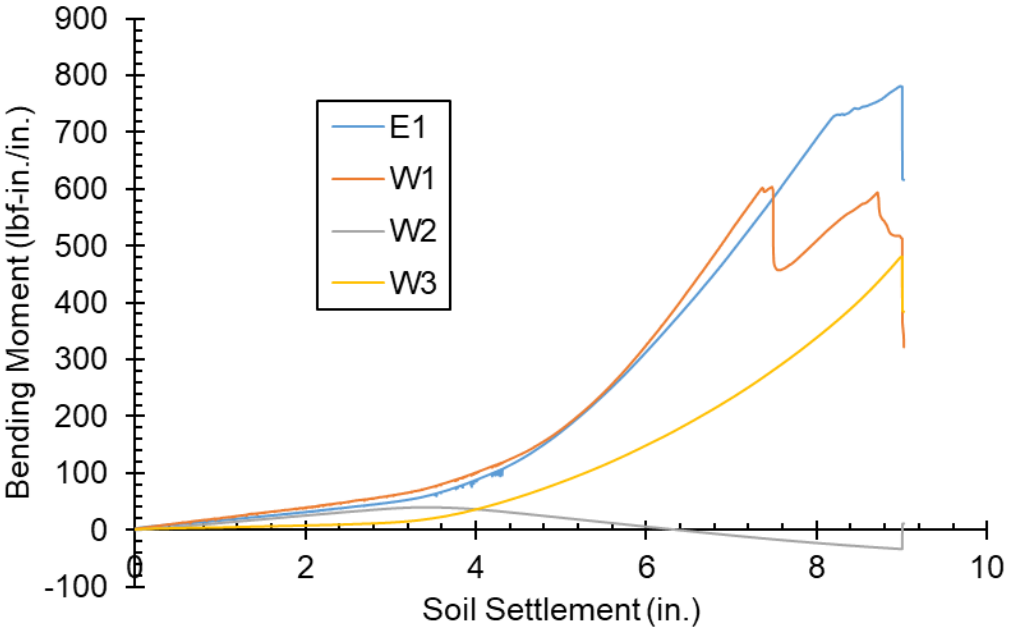

Figure 3-21 : Circumferential bending moment distribution.

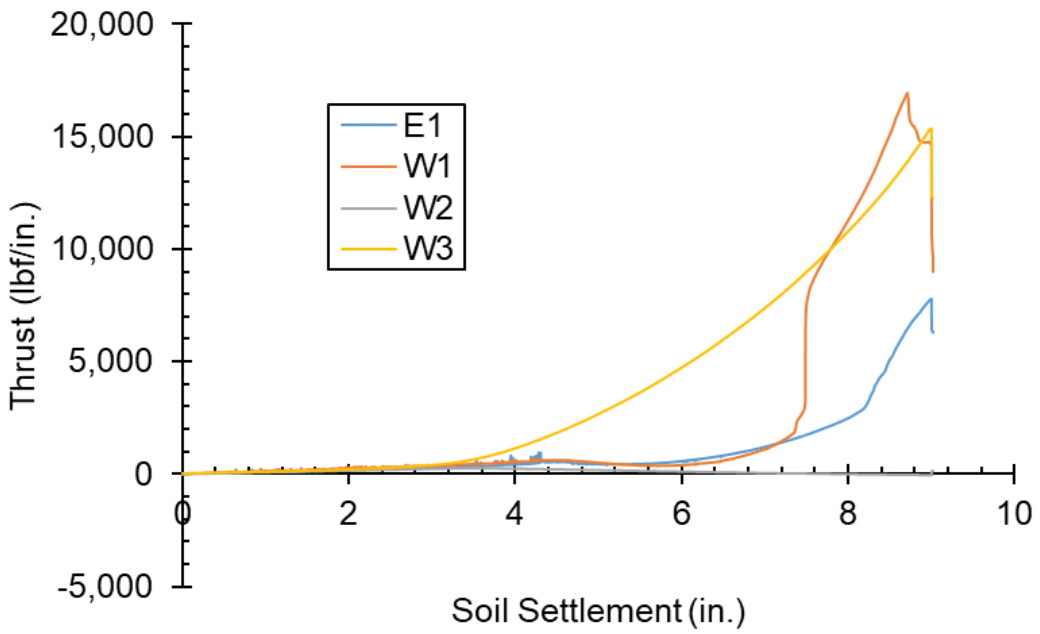

Figure 3-22: Circumferential thrust distribution.

Comparison with Intact CMP

After performing the tests on intact and invert-cut CMP, it is immediately obvious that the loss of invert has significantly reduced the capacity of the system. While the increase in load pad size was made to prevent bearing failure of soil, the low load resistance provided by the invert-cut CMP suggests that the CMP will probably have failed first even for the smaller load pad.

Load deformation behavior for both soil and CMP was compared between the intact and invert cut cases. However, since the two tests had different load pad sizes, direct comparison between the forces could not be made. Instead, applied pressure was used to compare the two cases. There is a drastic difference in pressures that was taken by the system between intact and invert cut CMPs. There is a 91.1% decrease in the maximum pressure that could be taken by the system prior to CMP's failure. Additionally, the mode of failure is also different. In intact CMP, soil failed before the pipe and eventually, the pipe failed in buckling. However, for invert cut CMP, the CMP failed due to excessive deformation as the cut edges of the invert moved towards each other and eventually touched. Hence while the soil was seen as the limiting factor in intact CMP, the limiting factor was the CMP in case of invert cut CMP.

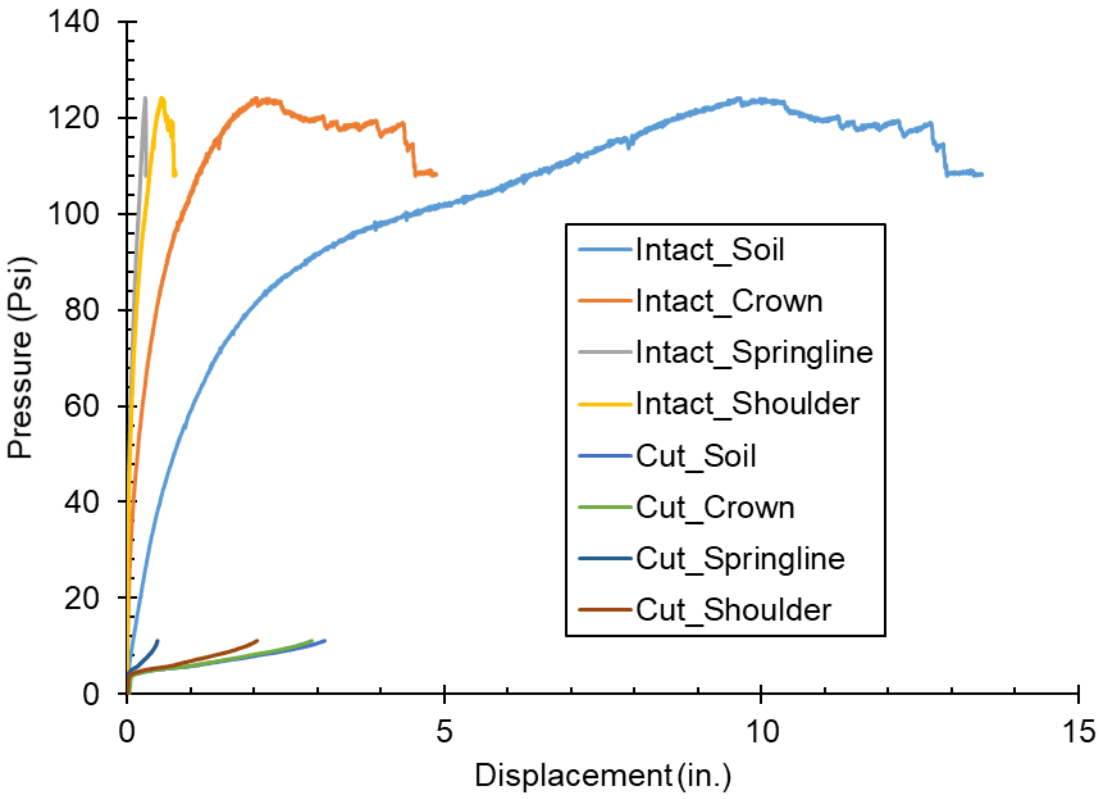

Figure 3-23: Comparison of load deformation capacity for soil.

3.9 Summary

After the first test on the intact CMP, it was observed that at a shallow cover of 2 ft, the full capacity of the side support from the soil could not be fully utilized with the CMP buckling at the crown, without significant deformations in the sides. This suggests that, in case of shallow cover, it is not the pipe that determines the performance limit, as is usually the case. Instead, it is the capacity of the cover soil that determines the failure limit. Hence, it seems vital that the cover soil be of good quality and with high strength if the full capacity of the pipe-soil interaction system is to be utilized, provided that the pipe itself is intact and free from any damage. It was also observed that the CMP behaved symmetrically about the vertical axis and the maximum values for bending moment and circumferential thrusts were located at the crown. Since the CMP failed by buckling at the top without significant deformations at the sides, the moments and thrusts at the top reduced after the buckling started while the moments and the thrusts at other locations kept rising over the course of the test.

Since bearing failure was seen in intact CMP, the size of load pad was increased for the test of invert cut CMP. The invert cut CMP could take significantly lower pressure as compared to the intact CMP. The invert cut CMP's load capacity increased significantly once the cut edges touched each other. However, the CMP experienced significant

deformation and reduction in diameter prior to this point. Hence, the system's failure was defined as the point at which the cut edges of the invert touched each other. Thrust and moments at the locations away from the crown were found to be much more significant than that for intact CMP. The maximum measured bending moment and thrust was observed at the shoulder location.

Chapter 4 FINITE ELEMENT ANALYSIS

4.1 Introduction

Finite element analysis, when used correctly, is an extremely valuable tool to observe the behavior of the various components of a complex system. It can serve both as a preliminary tool that can be used to design a suitable experimental plan and as a prediction tool that can be used to predict a system's behavior under varying conditions.

There are several finite element analysis tools that have been used in the past to model the behavior of buried culverts. Some of the more popular options are CANDE, Abaqus, Plaxis and ANSYS. In this study, Abaqus 6.14 has been used to model the behavior of the buried CMP. Abaqus is a powerful, multipurpose simulation tool that can be used to model a wide variety of systems (Dassault Systemes 2014). The high degree of control over the geometries, mesh and material interactions make Abaqus a suitable tool to model the system with complex geometry, in the form of CMPs and, complex interaction between parts of the model i.e., pipe-soil interaction.

4.2 Model Setup

The Abaqus model of the test consists of two main parts: the CMP and the surrounding soil. Due to the complex geometry of the CMP and the resulting complex contact surface with the soil, the parts geometry could not be created in Abaqus. Instead, both the parts were created in Fusion 360, a CAD software from Autodesk. Due to symmetry of the test setup, only half of the geometry was created and modeled to increase the efficiency and reduce the computation time of the model.

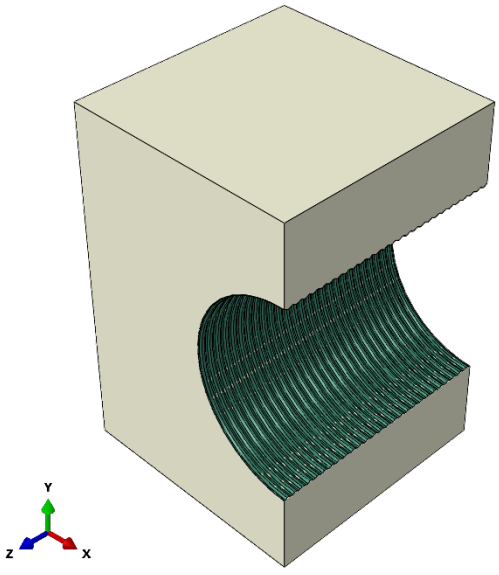

Figure 4-1: Model Setup

4.3 Load and Boundary Conditions

The model has an axis symmetric boundary about the Y-Z plane on the right (blue triangles). The sides of the model are restricted against horizontal movement (orange triangles). The bottom face of the model is restricted against vertical movement (orange triangles). No additional boundary conditions are applied to the CMP.

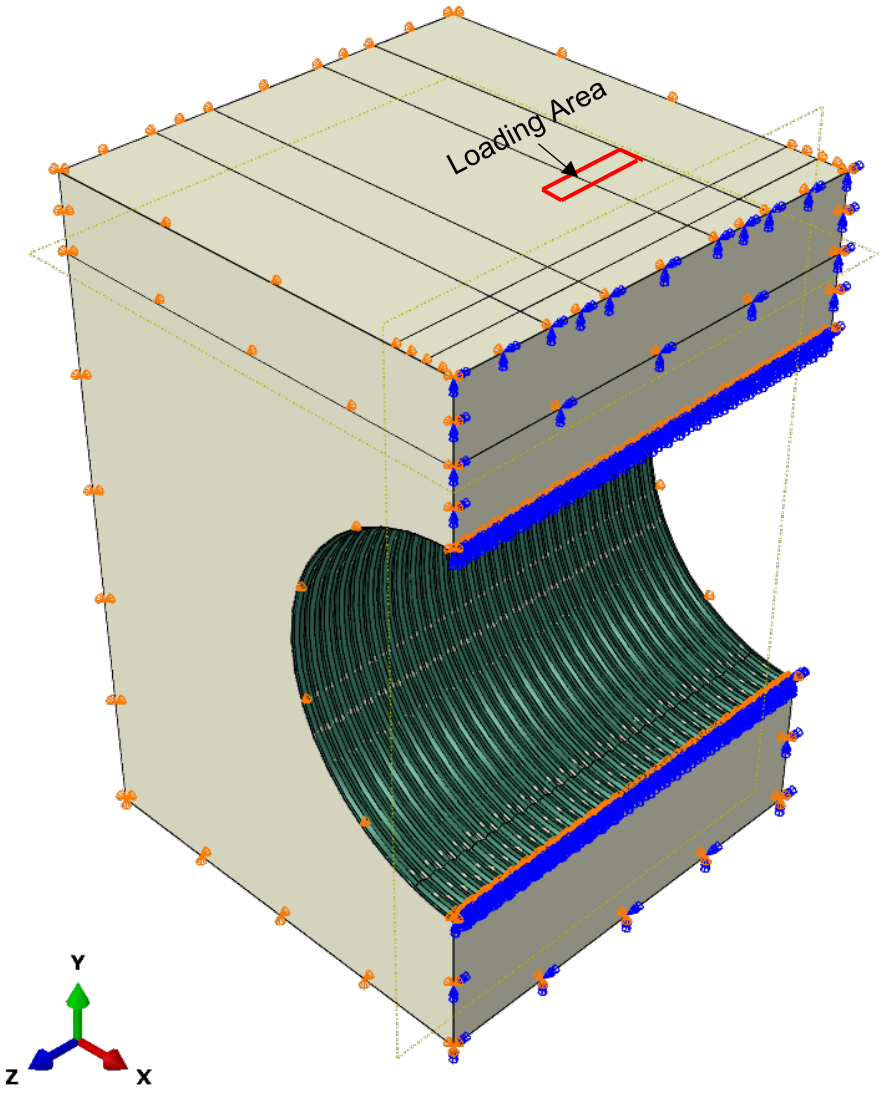

Figure 4-2: Boundary conditions

To reduce the number of parts, contact surfaces and hence the model complexity, load in the model is applied by providing a downward displacement of 5 in. at the contact area of the load pad in the actual test (red rectangle). To ensure simultaneous movement of all loaded nodes (simulating load transfer from rigid load pad), an equation constraint was used to relate all the nodes in the loading area to a central node such that any

movement in the central node was mirrored by all the nodes with the equation constraint. The displacement was then applied only to the central node.

4.4 Material Models

The model has two types of materials: the backfill soil and steel. This section describes the material models used in Abaqus to represent these materials.

4.4.1 Steel

The CMPs are made of corrugated steel sheets conforming to ASM 929 with yield strength 33 ksi and ultimate strength 45 ksi. The modulus of elasticity of the steel was 29,000 ksi. A regular elastic-plastic model available in Abaqus was used to model behavior of steel. Table 4-1 shows the properties of the steel used in Abaqus.

Table 4-1: Steel Properties in Abaqus

Property	Value
Density (lb./in^3)	0.284
Elastic Modulus (psi)	29,000,000
Poisson's Ratio	0.3
Yield Stress (psi)	33,000
Ultimate Stress (psi)	45,000

4.4.2 Soil

There are various soil models available in Abaqus to model the behavior of soil. In this study, the Drucker Pager model, which is a three-dimensional, pressure dependent model, has been used to model the soil behavior. There are two types of soil used in the model viz.: concrete sand and gravel. Table 4-2 shows the properties used for defining the behavior of the two soils.

Table 4-2: Soil properties used in Abaqus

Property	Sand	Gravel
Density (lb./in^3)	0.057	0.069
Elastic Modulus (psi)	720	1100
Poisson's Ratio	0.3	0.28
Friction Angle (°)	33	37
Dilation Angle (°)	1	2

4.5 Interaction

Abaqus allows the user to define different interaction models for the components of the model. In this model, the interaction between the pipe and soil surface is represented using the surface-to-surface contact where, the pipe is treated as the master surface while the soil is treated as the slave surface. A friction coefficient of 0.75 is defined between the CMP and soil and the contact is defined as a hard contact i.e., the pipe does not “pierce” the soil but displaces it.

4.6 Model Steps

The model is run in static condition. Analysis is done in three steps that represent different stages during the test. The following steps are followed in the model:

1. The first step is a geostatic step. In this step, the soil is allowed to reach its stable condition under the given boundary conditions. This step is required in almost any model that includes soil and activates the load due to self-weight of the soil. No interaction is defined between pipe and soil in this step.
2. In the second step, the pipe is activated i.e., the load due to self-weight of the pipe is defined. Interaction between pipe and soil is also defined in this step.
3. In the third and final step, external load is applied to the system.

4.7 Element Type and Mesh Sensitivity Analysis

Finite element modeling, while a very useful too, also has high potential for errors if not used carefully. Depending on the type and complexities of the model, different factors can influence the results obtained such that, two people modeling the same phenomenon may get entirely different results. One of these factors is the type of elements used to discretize the two parts and computation method used to obtain the solution. Due to complicated model geometry and limited computational power, a linear brick element was used. However, fully integrated linear brick elements are too stiff to accurately represent the bending of elements (Sun, 2006). This problem can be solved either by using higher order elements (significantly higher computational cost) or, by reduced integration which provides better flexibility to the elements. However, reduced integration has a problem of its own in that it can make the model excessively flexible. This phenomenon is called hourglassing and it must be properly controlled to obtain realistic results. Many commercial FEA codes, including Abaqus, usually have in-built functions to address this very issue. Hence, an eight-node linear brick element with reduced integration and hourglass control (C3D8R) was used to discretize the two parts in Abaqus.

The other major factor that affect the FEA results is the mesh size. Even when properties and interactions in the model are correctly defined, mesh size can cause big variation in results. Therefore, it is crucial to make sure that the model is mesh

independent. There are several parameters that can be used as error indicators to check the mesh sensitivity and numerical accuracy of the model.

The numerical accuracy of the model can be determined by checking for the total energy of the model. For a general static model in Abaqus, the total energy of the system is defined as:

$$\begin{aligned}\text{Total Energy} = {} & \Sigma\text{Total Internal Energy} + \Sigma\text{Total Elastic Contact Energy} \\ & - \Sigma\text{Total External Work} - \Sigma\text{Total Frictional Dissipation} \\ & - \Sigma\text{Total Contact Dissipation} = 0\end{aligned}$$

However, due to computational imperfections, this sum is not usually equal to zero and an error close to 1% is usually expected (DDS SIMULIA 2006) The total energy of the system was checked at various mesh sizes and for all sizes, the error percentage was less than 1% of the total internal and external energies, hence verifying the numerical accuracy of the model.

To determine the mesh sensitivity of the model, total energy, plastic strains, load-displacement for soil and pipe and the Von Mises stress for the pipe were compared among the mesh sizes of 3.4, 3, 2.4. For the soil, the differences in values of plastic strain and load-displacement didn't vary by a significant amount for mesh sizes 3.4, 3, 2.4. (Figure 4-3) Hence, a mesh size of 3.4 for soil was initially adopted to save computational time.

For pipe, the values of Von Mises stress and crown displacement had small differences for mesh sizes 3.4 and 3 however, plastic strains showed a higher value at mesh size 2.4. Hence, the pipe was checked for mesh sizes 2, 1.75, 1.5, 1, 0.75. For all cases, the value of Von Mises stress and crown displacements were virtually identical while the values of plastic strain were very close for sizes 2.4 to 1.5 but increased more for 1 and 0.75.

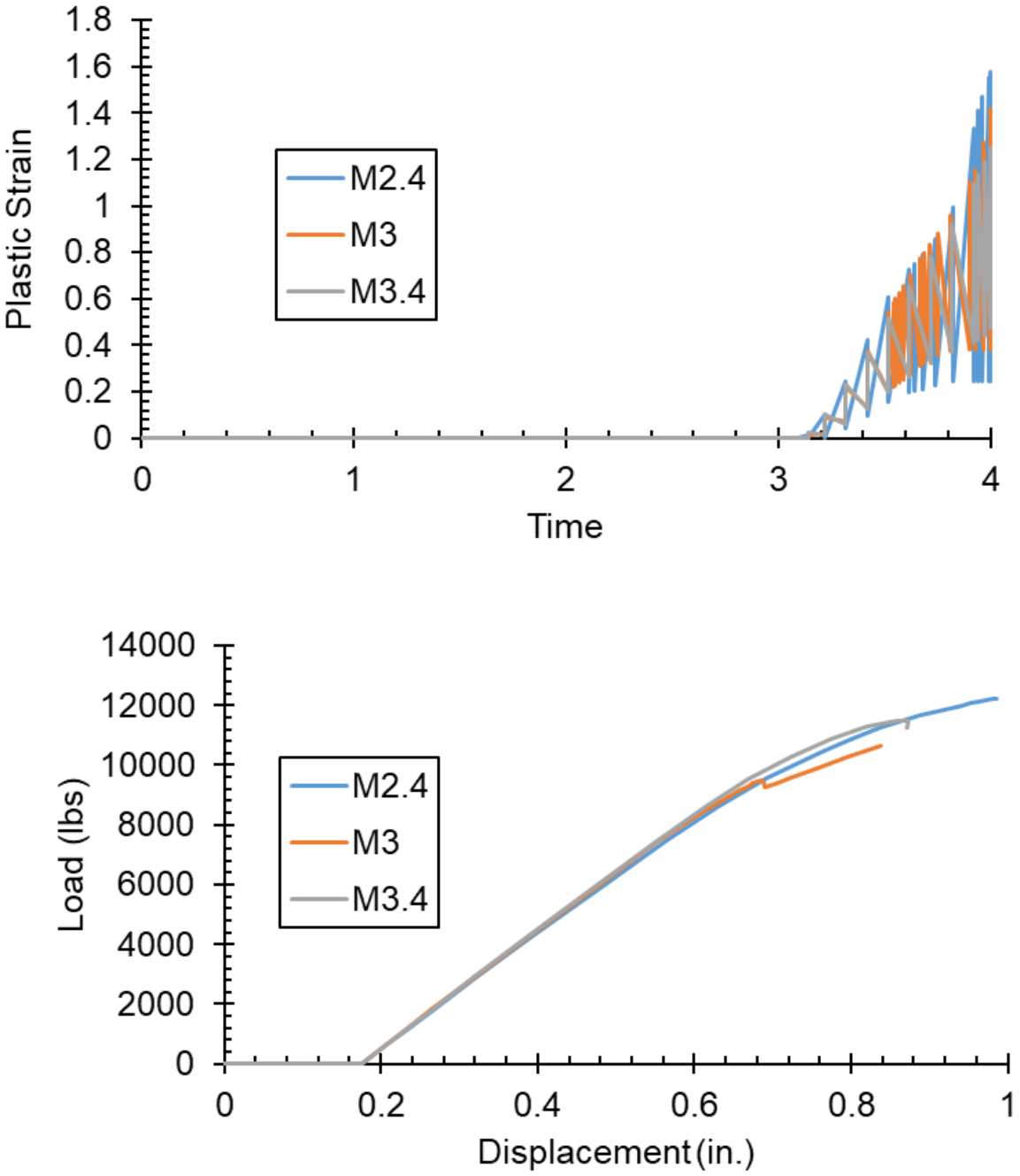

Figure 4-3: Plastic strain (top) and load-displacement (bottom) plot for soil.

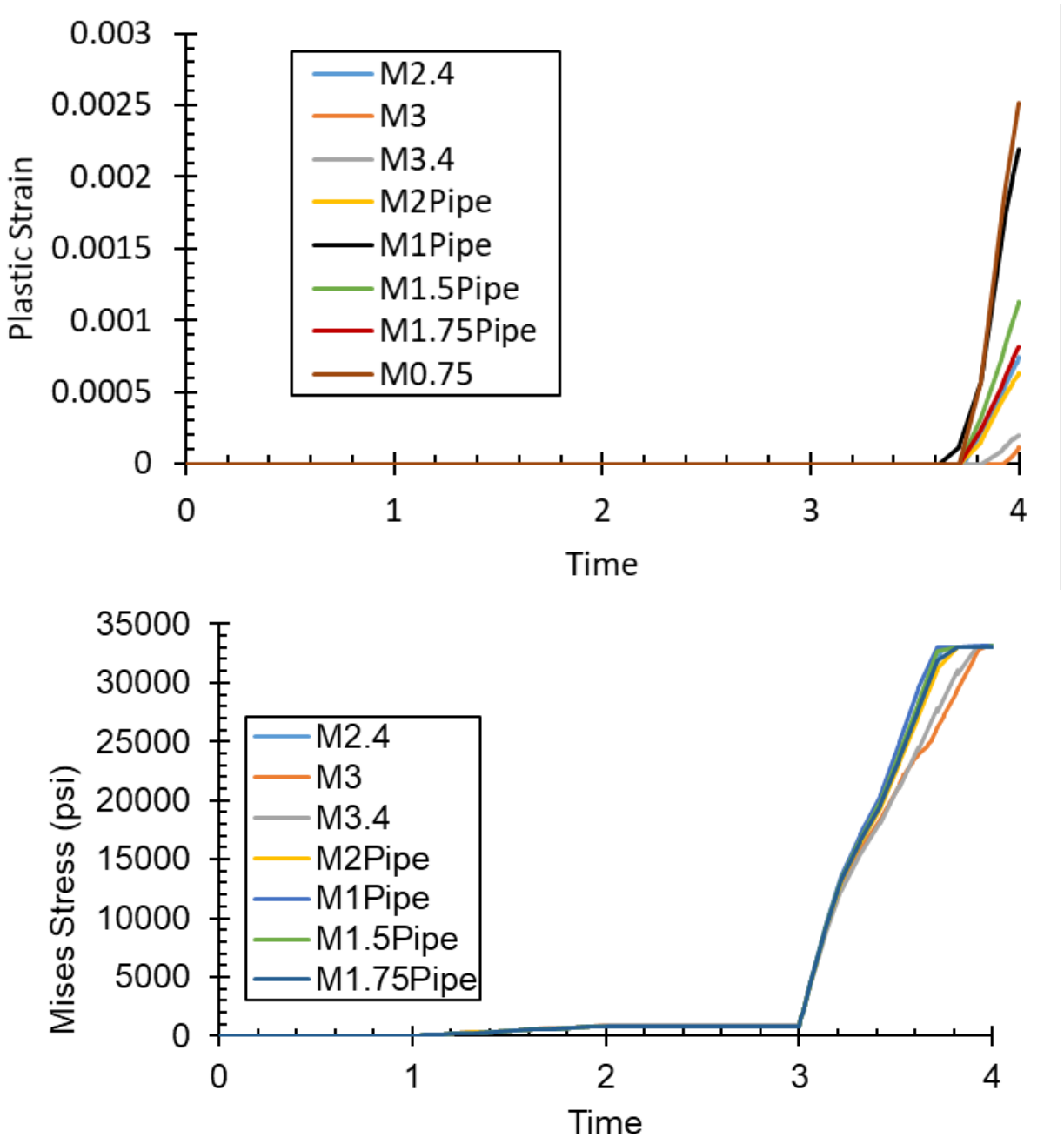

Figure 4-4: Von Mises stress (top) and plastic strain (bottom) in pipe.

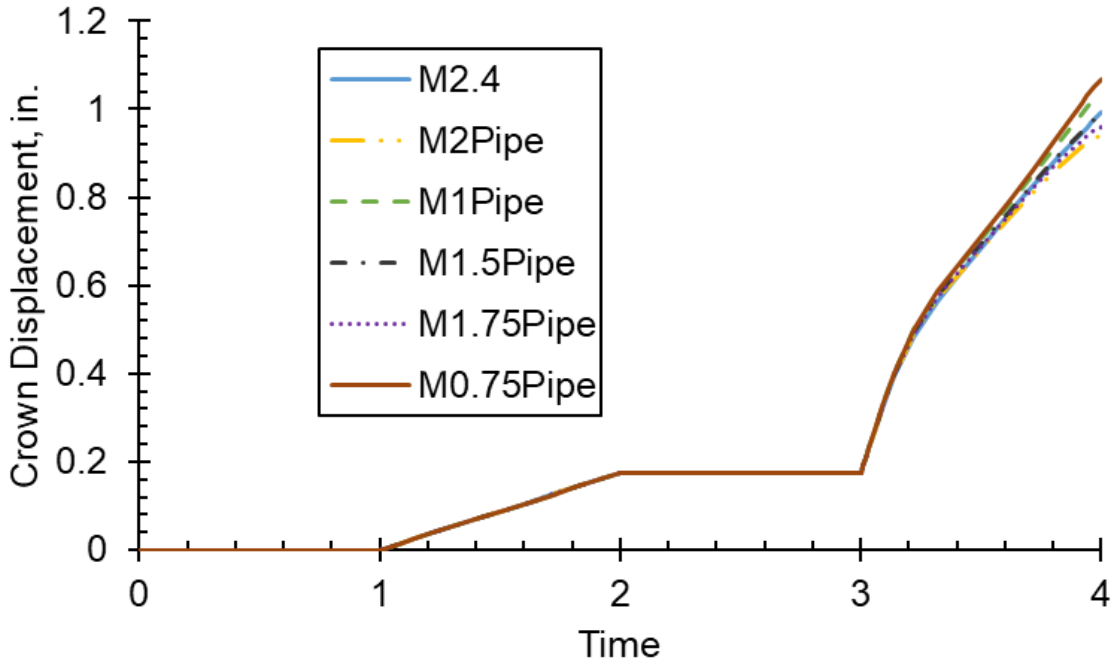

Figure 4-5: Crown displacement for varying mesh sizes.

Hence, a mesh size of 2.4 was deemed suitable for the CMP. To make the model computationally efficient, mesh size 2.4 was used for both soil and pipe.

4.8 Results and Discussion

4.8.1 Intact pipe

The FE element modeling of the laboratory test on intact CMP was performed using Abaqus according to the steps mentioned in previous sections. The FE model mimicked the experiment in that it also showed soil failure prior to significant deflection in the pipe (Figure 4-6). There is a significant plastic strain around the loaded area in the soil and the loaded itself has punched into the soil. This matches what was observed during the experiment as well.

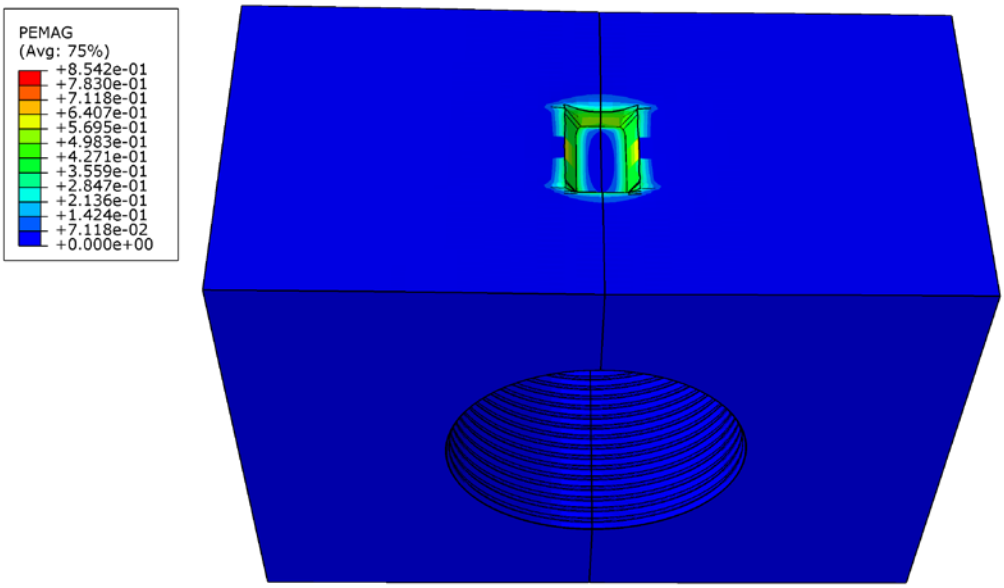

Figure 4-6: Plastic strain due to the soil failure in the loaded area.

The model also showed that at the end of the analysis, there was plastic strain developing at the pipe top, directly below the loaded area (Figure 4-7).

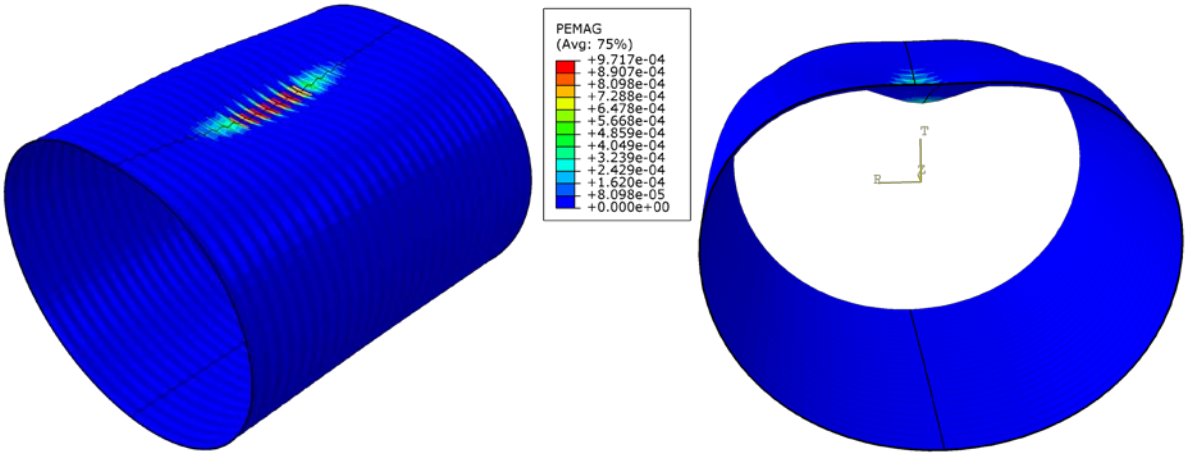

Figure 4-7: Plastic strain and deflection pattern in the CMP.

The CMP has exhibited buckling behavior in the model. There is also a slight settlement in the foundation/bedding layer (Figure 4-8). These observations prove that the FE model has, at least qualitatively, fairly represented the experimental test. The observed results were then compared with the results obtained from the experiment to obtain qualitative assessment of the test and FE model.

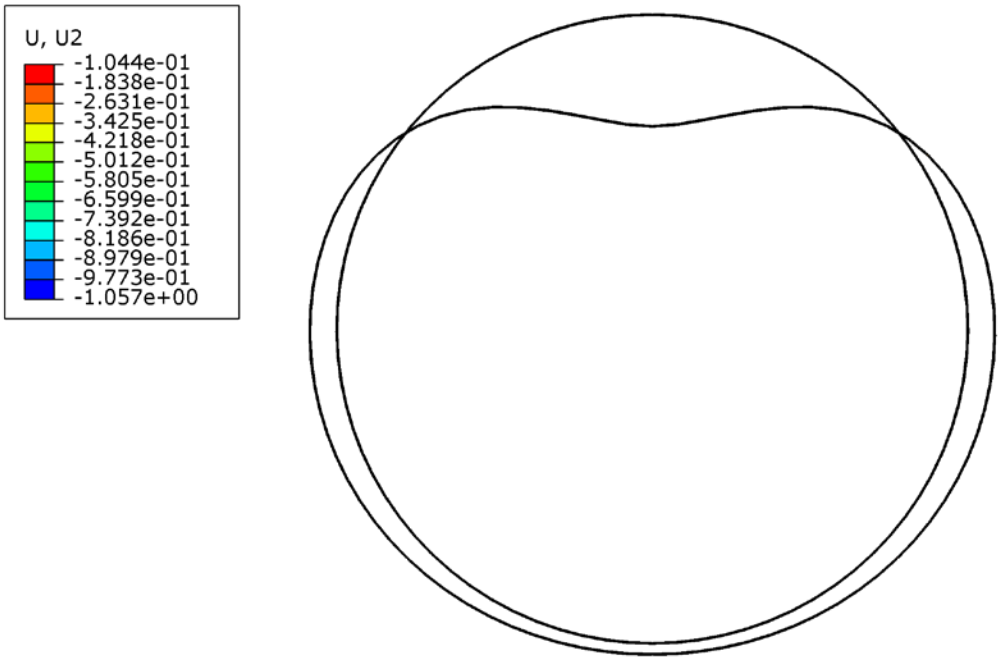

Figure 4-8: Buckling pattern observed in the CMP (scaled up).

Load-Displacement Plots

Load vs displacement plots were generated for both soil and pipe from Abaqus (Figure 4-9). The FE plots showed a good match with the experimental plots with a maximum of 8% difference in displacement of the soil observed. The failure of cover soil was also seen at a similar displacement value in both the model and experimental curves.

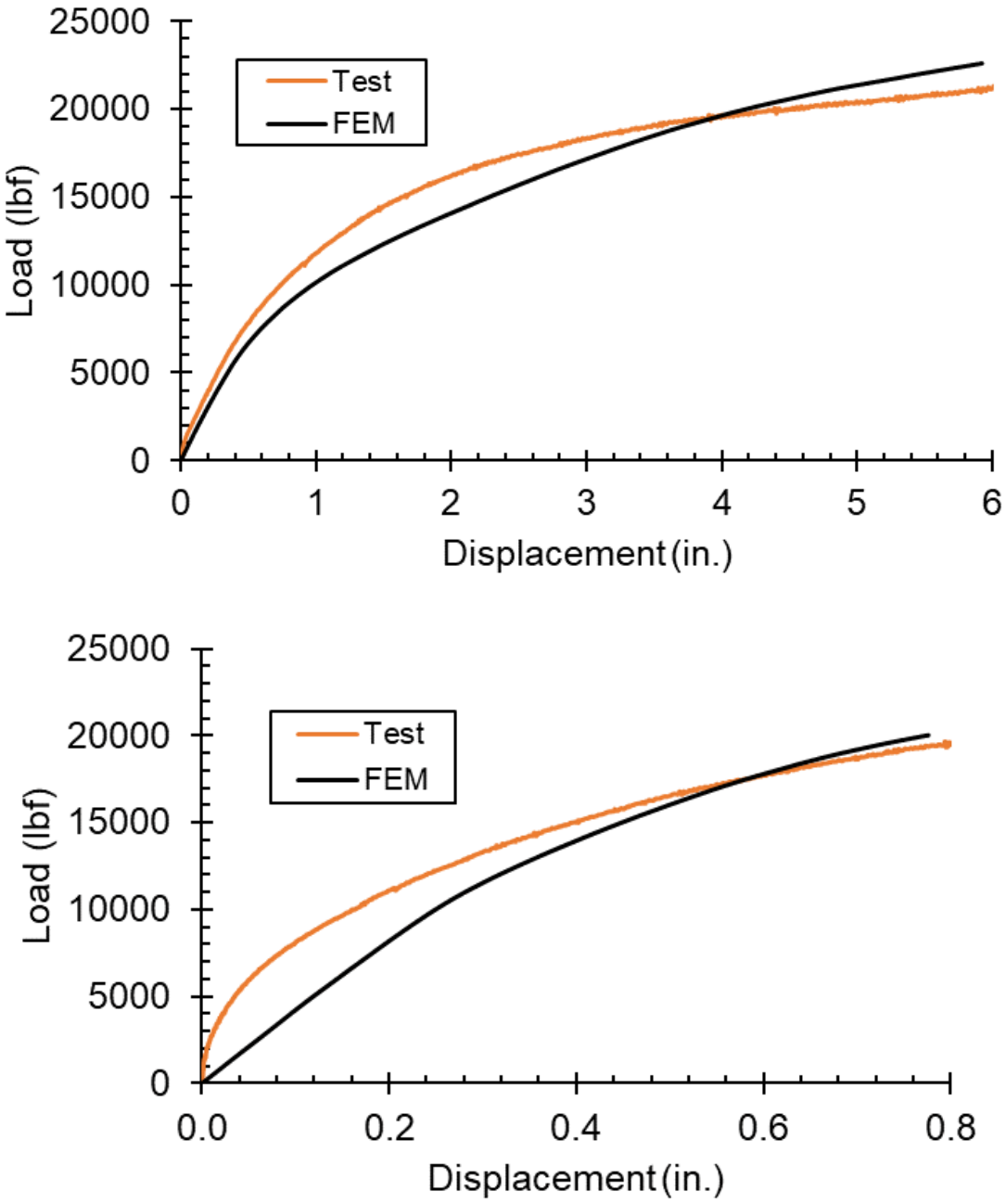

Figure 4-9: Load displacement plots for soil (top) and pipe crown (bottom) compared with experimental plots

Horizontal displacement of the pipe was obtained at the springline of the FE model. This was then compared with the displacement values obtained from the LVDT installed at the springline (Figure 4-10). The maximum difference of about 17% was observed between the FE model and experimental data.

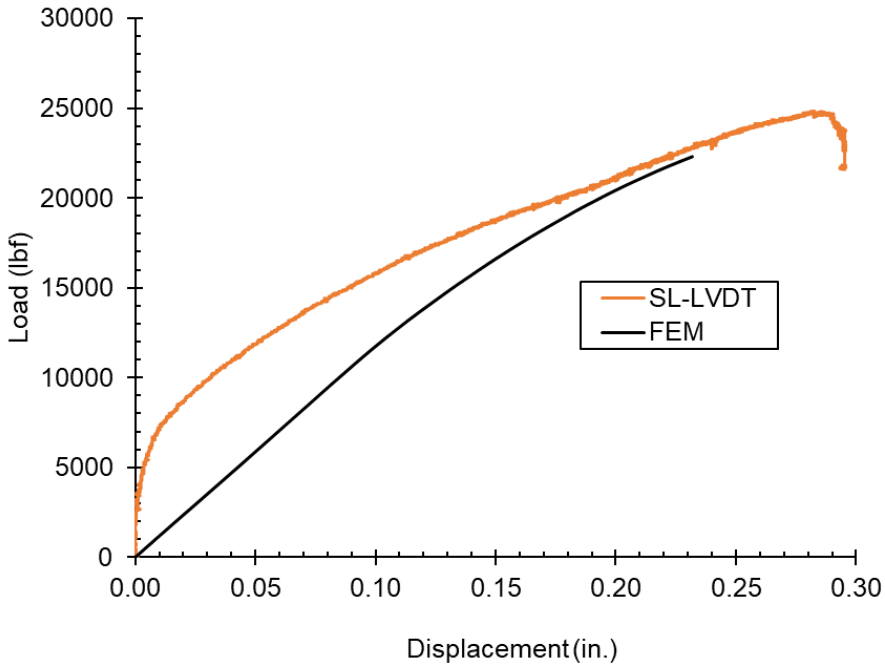

Figure 4-10: Horizontal displacement at springline.

After the cover soil failed, the experiment was continued and as the pipe took the load, the load displacement curve rose again and dropped after the pipe buckled. However, this second rise could not be modeled using FEM as once the cover soil fails, any further increase in load causes large displacements which cannot be defined by the soil model used and hence, the FE model fails to converge.

Strains, Bending Moment and Thrusts

Strains measured around the CMP showed that the highest value for strain was observed at the crown level. Hence, comparison was made for the strains at crest and valley of the corrugation at the top of the pipe observed during the test with the same obtained from the FE model (Figure 4-11). The FE model shows a good match with the strain observed at the top of the pipe. The trend of strain observed for both crest and valley is similar between the test and FE model. However, there is a greater variation between the measured and predicted strain observed at the crest of the corrugation.

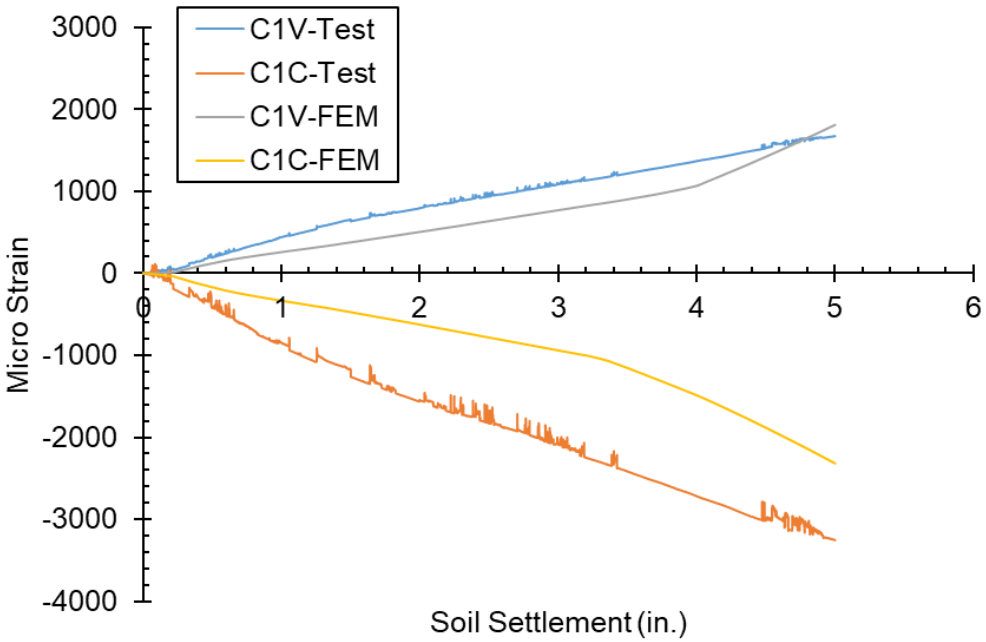

Figure 4-11: Comparison of strain observed at the top of the pipe.

The bending moment obtained from the finite element model at the end of analysis was compared with the bending moment obtained from the laboratory test at the similar state. Both bending moments and thrusts at the different location showed good match with the experimental results.

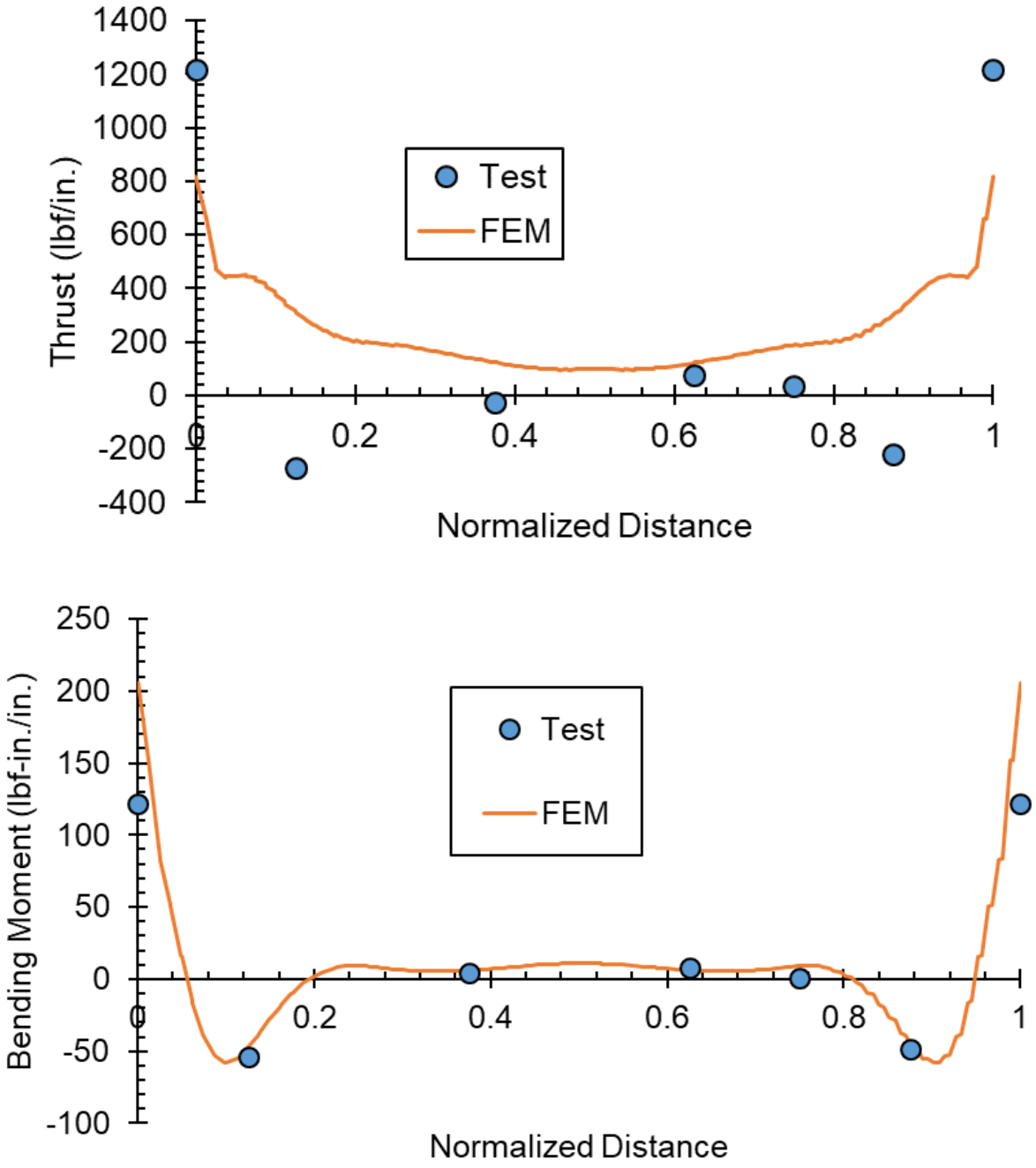

Figure 4-12: Circumferential thrust (top) and bending moment (bottom) distribution around the CMP predicted using FE model at 3 in. soil settlement.

Earth Pressure Distribution

The earth pressure variation at the crown level of CMP obtained from earth pressure cell was compared with the variation of earth pressure at the similar location in the FE model. The values were also compared with pressures estimated by AASHTO and 2:1 pressure distribution (Figure 4-13).

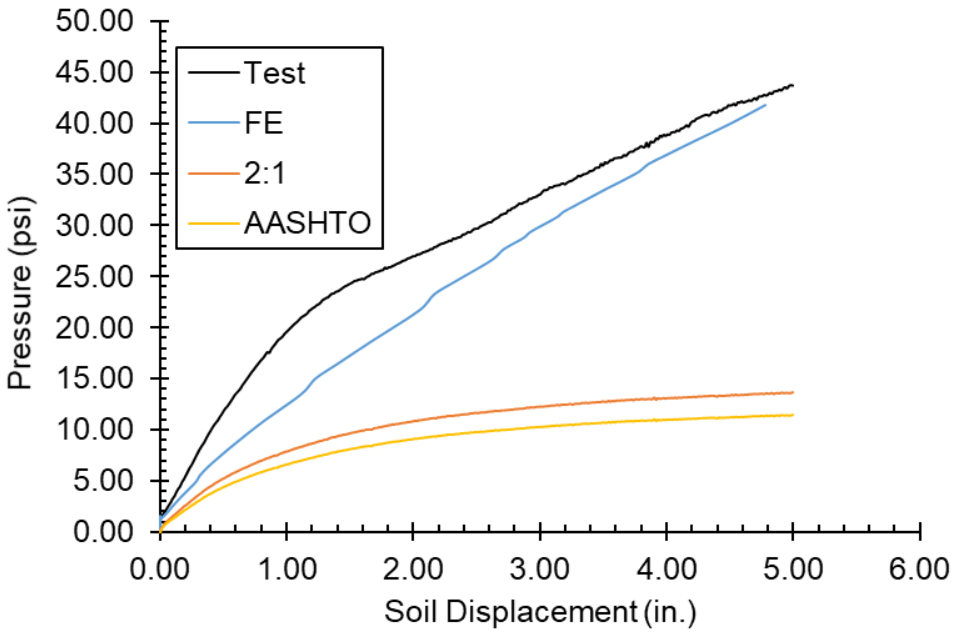

Figure 4-13: Earth pressure distribution at the crown level.

The FE model predicted the earth pressure variation at the crown with good accuracy. Both AASHTO and 2:1 method significantly underpredict the earth pressure at the crown level of the CMP. Comparison was not made for earth pressures at springline and invert level as the regions showed extremely low measure pressure and the accuracy of the earth pressure cells at this range in low.

4.8.2 Invert-cut pipe

Once the FE model was used to study the test behavior of intact pipe. The model was extended to study the behavior of invert cut CMP. Again, the model followed the test sequence in that the CMP was buried and allowed to stabilize under intact condition. After this, the invert of the CMP was removed, and then external load applied through the contact area of the bigger load pad. Invert removal in the FE model was simulated using interaction command “model change” after step 2 (section 4.6 above) which then removed the elements in the invert. External load was then applied after invert removal.

It was observed that, once the invert of the CMP was removed, sudden movement occurred as the CMP tried to redistribute the soil pressures and regain stability. This resulted in the gap in invert being reduced as the CMP moved inwards. This horizontal movement was accommodated by the settling of the pipe’s crown. At this state, plastic strain was seen in the soil at springline while, the pipe itself did not have any plastic strains (Figure 4-14). However, the magnitude of movement was smaller as compared to the movement seen during the test with only 1.8 inch of horizontal movement seen in the FE model (Figure 4-15).

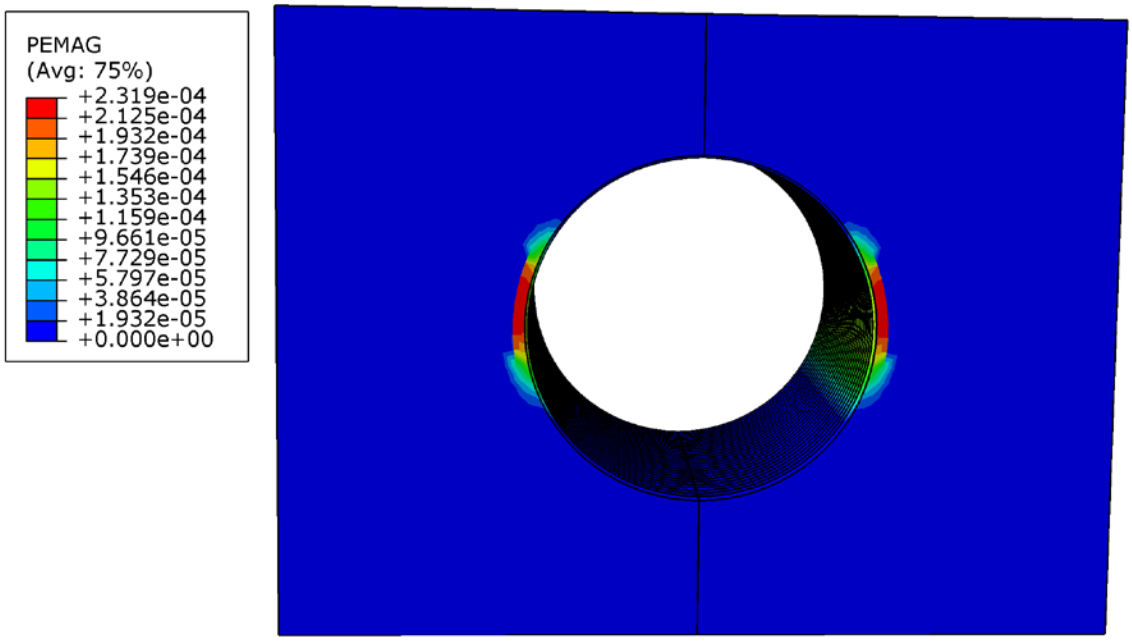

Figure 4-14: Plastic strain at the springline level in soil after invert is removed.

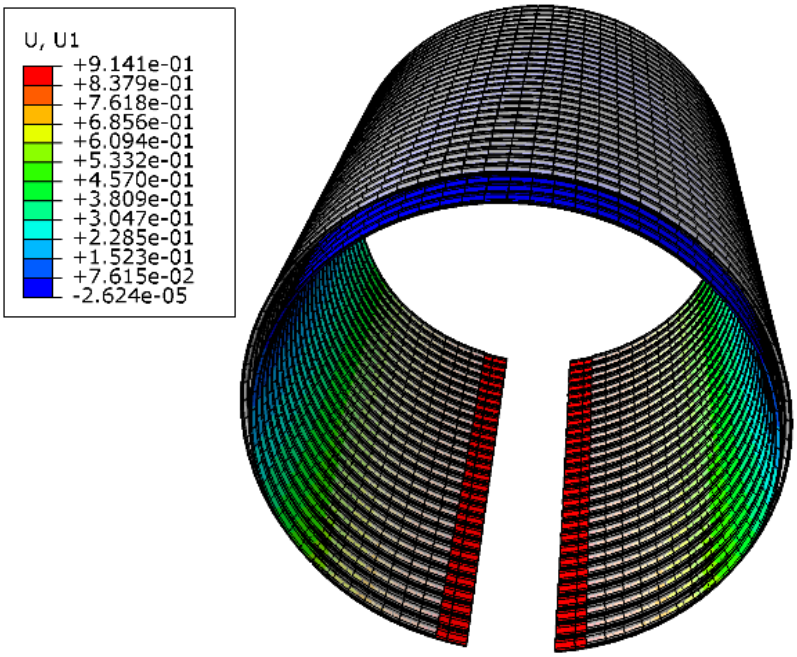

Figure 4-15: Horizontal displacement of the pipe after invert removal.

Once external load was applied to the system, the topsoil behaved in a similar manner as the case of intact CMP. Plastic strain was seen in the soil around the load pad while the pipe did not show any plastic strain (Figure 4-16). However, the total extent of

soil settlement was low. Only 3 inches of total settlement could be applied to the model prior to failure.

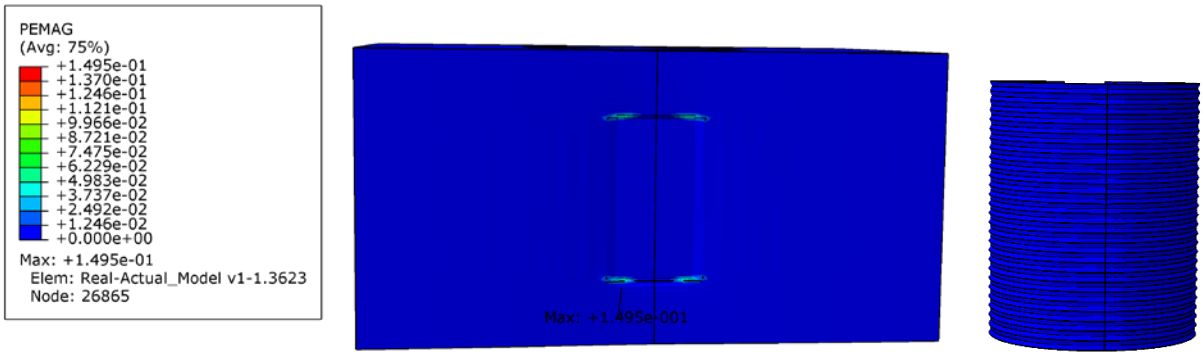

Figure 4-16: Plastic strains in soil and CMP at 5 in. soil settlement.

For 3 in. displacement, the soil around the loading area undergoes plastic deformation. However, no plastic deformation is observed in the pipe. Instead, significant horizontal movement is observed in the haunch region (Figure 4-17). At this state, a maximum vertical and horizontal deflection of 2.72 in. and 2.73 in. was observed at the crown and haunch respectively.

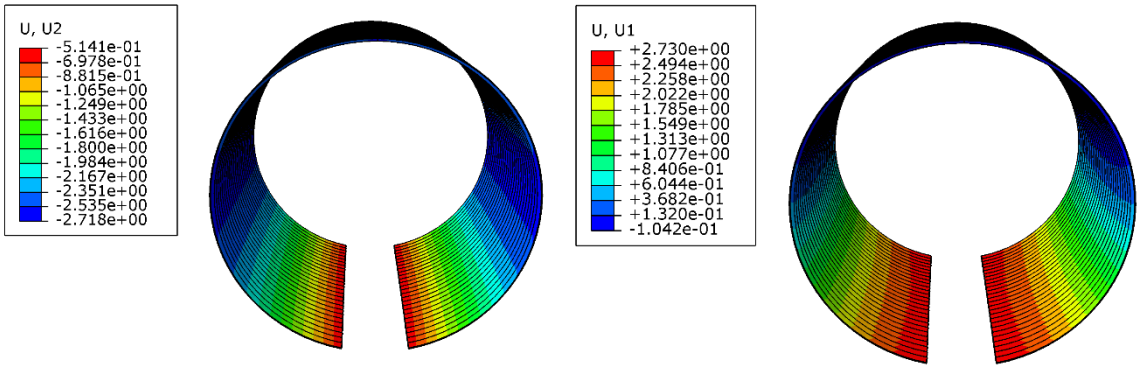

Figure 4-17: Vertical and horizontal deformation of invert-cut CMP.

While the cut edges of the invert touched in the test at the soil settlement close to 3.5 inches, the FE model still shows a significant gap remaining in the invert. As a result, the magnitude of deformations at crown and springline predicted by the FE model was lower than the actual test.

Load-Displacement Plots

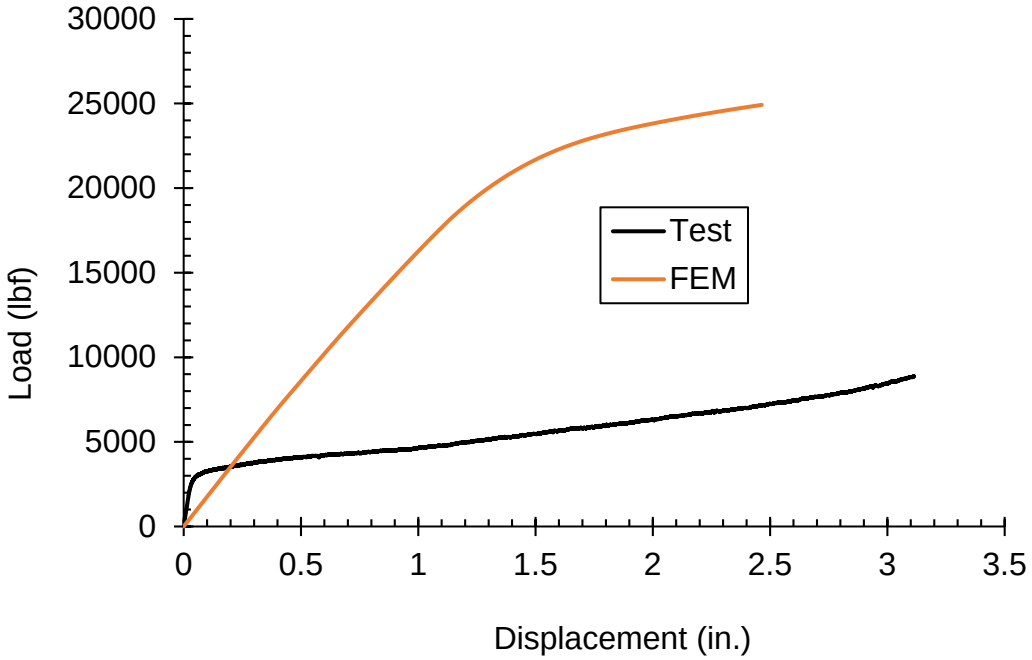

Figure 4-18: Load displacement plot for soil under applied load.

Load displacement curves were plotted for both soil and pipe under the applied load and compared with the plots obtained from the test. The FE model has significantly over predicted the strength of the invert cut CMP. For similar values of soil settlement, the ultimate load taken by the system is over two times higher than the maximum load seen in the test prior to the cut edges coming into contact (Figure 4-18).

The invert cut CMP has required significantly higher load to get the same deformation as that observed in the test. The springline of the CMP shows approximately 88% less horizontal movement than that observed in the test. Similarly, the total displacement of the cut edges is approximately 4 inches i.e., the gap in the invert of the CMP hasn't been closed, which wasn't the case observed in the test.

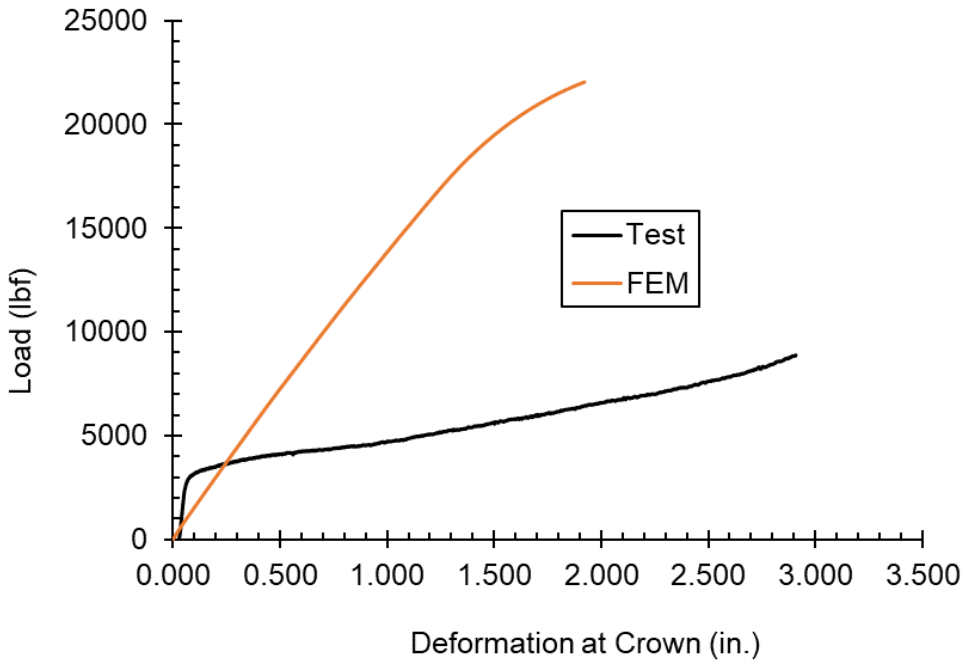

(a)

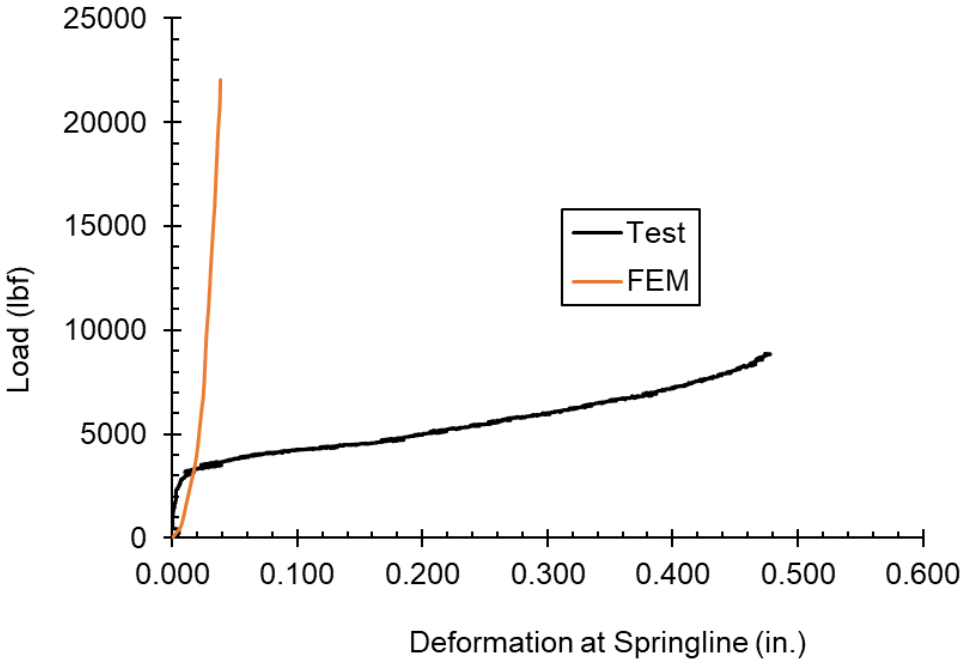

(b)

Figure 4-19: Change in vertical and horizontal diameter at: (a) Crown, (b) Springline of invert cut CMP.

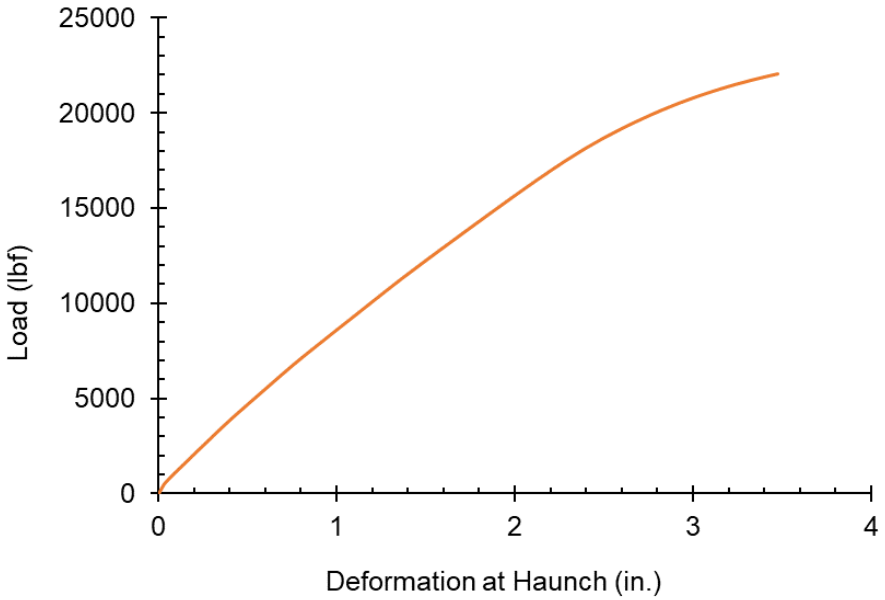

Figure 4-20: Deflection at the haunch region under applied load.

Earth Pressure Distribution

Comparison of earth pressure around the CMP was made to check for the discrepancies between the model and the test results. It is observed that the FE model seems to predict the vertical stress at crown level fairly well. However, the horizontal stress at the springline levels show a bigger difference. The horizontal stress in the FE model remains fairly constant as the load is applied however, the horizontal stress in the test increases with time (Figure 4-21).

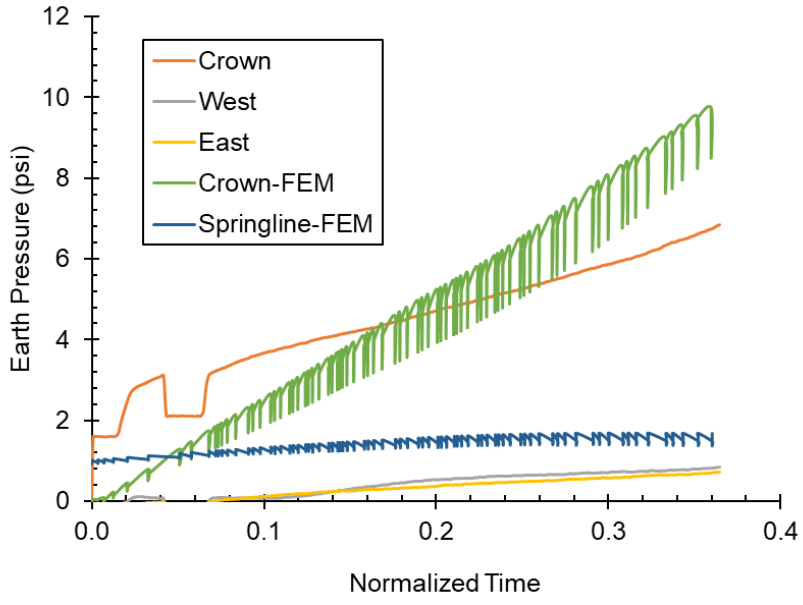

Figure 4-21: Distribution of earth pressure around the CMP.

This distribution suggests that the FE model has not been able to accurately represent the change in pressure states around the CMP as the soil flows after invert removal. This might also be the reason for the discrepancies seen in the CMP between FE model and the test. Hence, a constitutive model that can represent the flow behavior of the soil might be needed to improve the predictions for invert cut CMP.

4.9 Summary

Finite element modeling was done for the tests on intact and invert cut CMPs. For intact CMP, the pipe failed through local buckling at the crown, directly beneath the loaded area. The FE model showed good performance in predicting the deflections, moments and thrusts in the CMP. The load at soil failure was predicted to within 5% of the load obtained from experimental test. However, due to the failure of cover soil, the model was unable to predict the load at ultimate localized buckling of the pipe.

For invert cut CMP, the failure mode was excessive reduction in overall diameter of the CMP as the cut edges of the invert touched each other. The invert cut FE model gave a fair qualitative representation of the test behavior but overpredicted the magnitude of forces and deformations. The distribution of earth pressure obtained from the FE model seems to suggest a different constitutive model that can represent the flow behavior of soil after invert removal might have to be used to represent the plasticity of soil and thus improve the finite element model.

Chapter 5 CONCLUSIONS AND RECOMMENDATIONS

5.1 Conclusions

After the detailed analysis of the experimental results and finite element modeling, the following conclusions can be drawn:

1. Shallow soil cover was found to be a limiting parameter for a load pad with the same size as standard H20.
2. At above condition, the full capacity of the pipe due to the support from the surrounding soil could not be fully utilized.
3. The failure mode for the intact pipe was found to be buckling failure, and not the failure due to excessive reduction in diameter or failure at seams of the corrugated plate.
4. However, even at this shallow cover, the system could comfortably take the H20 design load of 16,000 lbs.
5. The finite element model was found to predict the system response fairly well.
6. However, due to failure of soil cover prior to pipe buckling, large displacements occurred in the model, which couldn't be defined using the soil model. This lead to the model's failure to converge and hence the model couldn't represent the second rise and peak seen after the soil failed during the experiment.
7. For invert cut CMP, the failure mode was excessive deformation. This deformation was heaviest at the location of the removed invert with the CMP moving inwards to reduce the gap and eventually touching each other.
8. The pressure taken by the invert cut CMP was significantly lower as compared to the pressure taken by intact CMP. A 91% reduction in stress carrying capacity was observed.
9. The resistance to load offered by the invert-cut CMP prior to the meeting of cut edges was small and even though this resistance increased significantly once the cut edges met, this happened after a big deformation and hence could not be considered as the actual capacity of the invert cut CMP.
10. A total loss of ring stiffness due to invert removal was seen as the critical performance limit for invert cut CMP, even at shallow cover.

5.2 Recommendation for future studies

The following points can be considered as possible areas for future studies.

1. Similar tests can be run at deeper cover to obtain the behavior under more realistic condition as culverts aren't supposed to be subjected to such shallow cover for regular operation.
2. The culverts can be loaded using the same approach and once certain performance criteria are crossed, the pipes can be repaired using different spray applied liners to obtain a more accurate data on the strength/capacity increased by such liners on damaged culverts.

3. Similar laboratory tests can also be conducted for arch, elliptical and box culverts to obtain a complete picture about how different culverts are expected to behave during similarly challenging conditions.
4. Similar tests can also be conducted using different loading schemes (e.g., tandem axle) and monitored at several sections in addition to the loaded section. This will provide more certainty on which section is more critical when loading.
5. The finite element models used can be improved upon by developing an approach that can remove the failed elements so as to avoid large displacements and hence obtain the complete load-deflection plot for the tests.
6. Different constitutive models can be used to represent the plasticity of soil to better represent the soil flow at invert removal and hence improve the FE model's accuracy.

REFERENCES

AASHTO. (2002). *Standard Specifications for Highway Bridges*. AASHTO.

AASHTO. (2017). *AASHTO LRFD Bridge Design Specifications*. *American Association of State Highway and Transportation Officials*, AASHTO, Washington, DC.

Arnoult, J. D. (1986). *Culvert Inspection Manual*. Federal Highway Administration (FHWA).

Arockiasamy, M., Chaallal, O., and Limpeteeprakarn, T. (2006). “Full-Scale Field Tests on Flexible Pipes under Live Load Application.” *Journal of Performance of Constructed Facilities*, 20(1), 21–27.

ASTM. (2008). *ASTM D2412-11 - Standard Test Method for Determination of External Loading Characteristics of Plastic Pipe by Parallel-Plate Loading*. *ASTM International*, ASTM.

ASTM. (2015). *ASTM D2850-15 Standard Test Method for Unconsolidated-Undrained Triaxial Compression Test on Cohesive Soils*. *ASTM International*, ASTM.

ASTM. (2016). *ASTM F1216- Standard Practice for Rehabilitation of Existing Pipelines and Conduits by the Inversion and Curing of a Resin-Impregnated Tube*. ASTM.

ASTM. (2017). *ASTM D1633 Standard Test Methods for Compressive Strength of Molded Soil-Cement Cylinders*. *ASTM International*, ASTM.

ASTM. (2019). *ASTM C497-19 Standard Test Methods for Concrete Pipe , Concrete Box Section, Manhole Sections , or Tile*. *ASTM International*, ASTM.

Ballinger, C. A., and Drake, P. G. (1995). *Culvert Repair Practices Manual Volume 1*. Federal Highway Administration (FHWA).

Bayoglu Flener, E. (2009). “Testing the Response of Box-Type Soil-Steel Structures under Static Service Loads.” *Journal of Bridge Engineering*, 15(1), 90–97.

Becerril García, D., and Moore, I. D. (2015). “Performance of deteriorated corrugated steel culverts rehabilitated with sprayed-on cementitious liners subjected to surface loads.” *Tunnelling and Underground Space Technology*, 47, 222–232.

Bergeson, K., Jahren, C., Wermager, M., and White, D. (1998). *Embankment Quality: Phase 1 Report*. Iowa State University.

Campbell, A. R. (2018). “Three-Dimensional Finite Element Modelling of Corroded Corrugated Metal Pipe Culverts.” Dalhousie University.

Crosby, M. K. A. Y. (2003). “Finite Element Analysis of a Laboratory Soil Box Test Facility.” University of Florida.

Darabnoush Tehrani, A. (2016). “Finite Element Analysis for ASTM C-76 Reinforced Concrete Pipes with Reduced Steel Cage.” University of Texas at Arlington.

Dassault Systemes. (2014). “Abaqus/CAE.” Dassault Systemes.

DDS SIMULIA. (2006). *Getting Started with ABAQUS/Explicit: Keywords Version*.

DEWCON Infrastructure Rehabilitation. (2019). “Pipe Slip Lining.” *DEWCON Infrastructure Rehabilitation*, <https://www.dewconinc.com/services/slip-lining> (Jun. 30, 2019).

Drnevich, V. P., and Evans, A. C. (2007). *A Study of Effective Soil Compaction Control of Granular Soils*.

El-Sawy, K. M. (2003). “Three-dimensional modeling of soil-steel culverts under the effect of truckloads.” *Thin-Walled Structures*, 41(8), 747–768.

El-Taher, M., and Moore, I. D. (2008). “Finite Element Study of Stability of Corroded Metal Culverts.” *Transportation Research Record: Journal of the Transportation Research*

Board, 2050(1), 157–166.
Elshimi, T. M. (2011). “THREE-DIMENSIONAL NONLINEAR ANALYSIS OF DEEP-CORRUGATED STEEL CULVERTS” Queen’s University.
Girges, Y., and Abdel-Sayed, G. (1995). “Three-dimensional analysis of soil – steel bridges.” *Canadian Journal of Civil Engineering*, 22(6), 1155–1163.
Howard, A. K. (1972). “Laboratory Load Tests on Buried Flexible Pipe.” *Journal / American Water Works Association*, 64(10 Pt 1), 655–662.
Katona, M. G., and Akl, A. Y. (1978). “Analysis and Behavior of Buried Culverts with Slotted Joints.” *Transportation Research Record*, 22–32.
Kouchesfehani, Z. K., Tehrani, A. D., Najafi, M., Syar, J. E., and Kampbell, E. (2019). “Adding Additional Reinforcement to Improve the Structural Performance of Spray Applied Pipe Lining Rehabilitation Technology: A Review.” *Pipelines 2019*, 10–23.
Kunecki, B., and Kubica, E. (2004). “Full-scale laboratory tests and FEM analysis of corrugated steel culverts under standardized railway load.” *Archives of Civil and Mechanical Engineering*, Vol. 4(December), 41–53.
Mai, V. T. (2013). “Assessment of Deteriorated Corrugated Steel Culverts.”
Mai, V. T., Hoult, N. A., and Moore, I. D. (2013). “Effect of Deterioration on the Performance of Corrugated Steel Culverts.” *Journal of Geotechnical and Geoenvironmental Engineering*, 140(2), 04013007.
Mai, V. T., Hoult, N., and Moore, I. (2018). “Numerical evaluation of a deeply buried pipe testing facility.” *Advances in Structural Engineering*, 21(16), 2571–2588.
Mai, V. T., Moore, I. D., and Hoult, N. A. (2014). “Performance of two-dimensional analysis: Deteriorated metal culverts under surface live load.” *Tunnelling and Underground Space Technology*, Elsevier Ltd, 42, 152–160.
Masada, T. (2017). *Structural Benefits of Concrete Paving of Steel Structural Benefit of Concrete Paving of Steel Culvert Inverts*.
Matthews, J. C., Simicevic, J., Kestler, M. A., and Piehl, R. (2012). *Decision Analysis Guide for Corrugated Metal Culvert Rehabilitation and Replacement Using Trenchless Technology*.
McGrath, T. J., Katona, M. G., and Goddard, J. B. (2018). “Culverts and Soil – Structure Interaction: 25 Years of Change and a Twenty-Year Projection.” *Transportation Research Board*, (E-C229).
Miliken Infrastructure Solutions. (2016). “Culvert Repair: Culvert Complications.” *Storm Water Solutions*.
Moore, Ian D. , Becerril Garcia, D. (2015). “Ultimate Strength Testing of Two Deteriorated Metal Culverts Repaired with Spray-On Cementitious Liners.” *Journal of Transportation Research Board*, (2522), 139–147.
Moore, I. D., and Brachman, R. W. (1994). “Three-Dimensional Analysis of Flexible Circular Culverts.” *Journal of Geotechnical Engineering*, 120(10), 1829–1844.
Najafi, M., and Gokhale, S. B. (2005). *Trenchless technology: pipeline and utility design, construction, and renewal*. McGraw-Hill.
National Corrugated Steel Pipe Association. (2008). *Corrugated Steel Pipe Design Manual*. National Corrugated Steel Pipe Association.
Regier, C., Hoult, N. A., and Moore, I. D. (2016). “Laboratory Study on the Behavior of a Horizontal-Ellipse Culvert during Service and Ultimate Load Testing.” *Journal of Bridge Engineering*, 22(3), 04016131.

Rinker Materials. (1994). “Corrugated Steel Pipe.”
Sargand, S. M., Khoury, I., Hussein, H. H., and Masada, T. (2018). “Load Capacity of Corrugated Steel Pipe with Extreme Corrosion under Shallow Cover.” *Journal of Performance of Constructed Facilities*, 32(4), 04018050.
Sharma, J. R., Najafi, M., Jain, A., and Marshall, D. (2013). “Use of Lime Stabilized Native Clayey Soils to Embed Large Diameter Steel Pipe.” *International Conference on Pipelines and Trenchless Technology 2012*, American Society of Civil Engineers (ASCE), 654–664.
Spangler, M. G. (1941). “The Structural Design of Flexible Pipe Culverts. Bulletin 153.” Iowa Engineering Experiment Station Ames, Iowa.
Sun, E. Q. (n.d.). *Shear Locking and Hourglassing in MSC Nastran, ABAQUS, and ANSYS*.
Syar, J. E., Najafi, M., Kouchesfehani, Z. K., Tehrani, A. D., and Korky, S. (2019). “Use of Spray Applied Pipe Linings as a Structural Renewal for Gravity Storm Water Conveyance Conduits.” *NAAST’s 2019 No-Dig Show*, NAAST, Chicago.
Tehrani, A. D., Kouchesfehani, Z. K., Najafi, M., Syar, J. E., and Kampbell, N. E. (2019). “Evaluation of Filling the Valleys of Corrugated Metal Pipes by Trenchless Spray Applied Pipe Linings.” *Pipelines 2019*, 84–94.
USBR. (1998). *Earth manual*. *USBR*, USBR.
Watkins, R. K., and Anderson, L. R. (1999). *Structural Mechanics of Buried Pipes*. CRC Press.
Watkins, R. K., and Spangler, M. G. (1958). “Some characteristics of the modulus of passive resistance of soil: A study in similitude.” *Highway Research Board Proceedings*, Transportation Research Board (TRB).
Whidden, W. R. (2009). *Buried Flexible Steel Pipe Design and Structural Analysis*. ASCE.